Influence of Space–Time Averaging on the Ocean–Atmosphere Exchange Estimates in the North Atlantic Midlatitudes

SERGEY K. GULEV

State Oceanography Institute, Moscow, Russia

(Manuscript received 7 March 1992, in final form 13 September 1993)

ABSTRACT

"Classical" and "sampling" methods of air–sea exchange estimates are considered. On the basis of meteorological observations at ocean weather stations in the North Atlantic, datasets of midlatitudinal experiments, and voluntary ship measurements calculations of sensible, latent, and momentum fluxes were obtained. The behavior of fluxes with increasing spatial- and temporal-averaging scales is explained. Simple parameterizations, using the space–time averaging influence on air–sea flux estimates, are produced. Some particulars connected with the role of different correlation terms are discussed.

1. Introduction

There are two main problems in the application of the bulk aerodynamic method for calculations of air–sea heat and momentum exchange on synoptic and climatological scales. One problem is connected with dynamical conditions and the influence of stratification on transfer and drag coefficients. The other is determined by the role of space–time averaging of hydrometeorological parameters. This problem is most important in midlatitudes and especially in frontal zones, where the extreme temporal variability of the atmosphere and strong SST gradients are observed. There are a number of articles (Kraus and Morrison 1966; Robinson 1966; Kondo 1972; Fissel et al. 1977; Esbensen and Reynolds 1981; Bortkovskiy 1983; Wright and Thompson 1983; Thompson et al. 1983; Marsden and Pond 1983; Larin and Panin 1985; Hanava and Toba 1987; Simmonds and Dix 1989; Gulev and Ukrainsky 1989) on the influence of temporal averaging of independent meteorological parameters on heat and momentum flux estimates. Most of the authors obtained visible differences between the "classical" and so-called sampling method of sea–air exchange estimates. However, Esbensen and Reynolds (1981) and Simmonds and Dix (1989) found good agreement between the monthly averaged heat fluxes and heat flux estimates, derived as the product of the monthly averaged wind speed and the monthly averaged sea–air temperature and humidity differences.

In contrast with temporal averaging, there are only a few studies connected with spatial averaging. Garstang (1965) was the first to give an evolution of intramonthly correlations over the tropical Atlantic. Reed (1985) calculated climatology of sea–air heat fluxes over the tropical Pacific and also found 3%–10% differences between sampling and classical estimates for monthly means in 2°latitude by 10°longitude areas. After that Mahrt (1987) proposed an approach for the calculation of grid-averaged surface fluxes for numerical models. He explored the relationship for exchange coefficients using the Louis (1979) scheme, originally chosen for continents, and tested his parameterization using data, collected also over the land. Some model studies focused on temporal averaging (Gavrilin and Monin 1969; Adamec and Elsbery 1984; Simmonds and Dix 1989), of course, indirectly take into consideration also spatial averaging, but they prefer to discuss their results in terms of temporal averaging. Several authors (Husby 1980; Weare and Strub 1981; Gilhousen 1987; Legler 1991) studied uncertainties in estimates of averaged meteorological parameters and energy fluxes, connected with inadequate sampling and annual and diurnal cycles. However, most of the estimates have been made for tropics of the Pacific Ocean. This study attempts to consider joint effects of spatial and temporal averaging in the North Atlantic midlatitudes on the basis of data for ocean weather stations and special scientific experiments.

2. Data

The data used in this study (Fig. 1) consisted of three-hourly sampled meteorological observations at Ocean Weather Stations B, C, D, and E for the period 1953–1974; one-hourly sampled observations at Ocean Weather Station C for the period 1975–1988; all voluntary meteorological observations in the northwest Atlantic for the last 10 years; and meteorological data

Corresponding author address: Dr. Sergey Gulev, % Prof. Sergey Lappo, Shirshov Institute of Oceanology, RAS, Krasikova St., 23, 117218, Moscow, Russia.
E-mail (OMNET): GULEV.BOBA
(INTERNET): gulev.boba@omnet.nasa.gov.

© 1994 American Meteorological Society

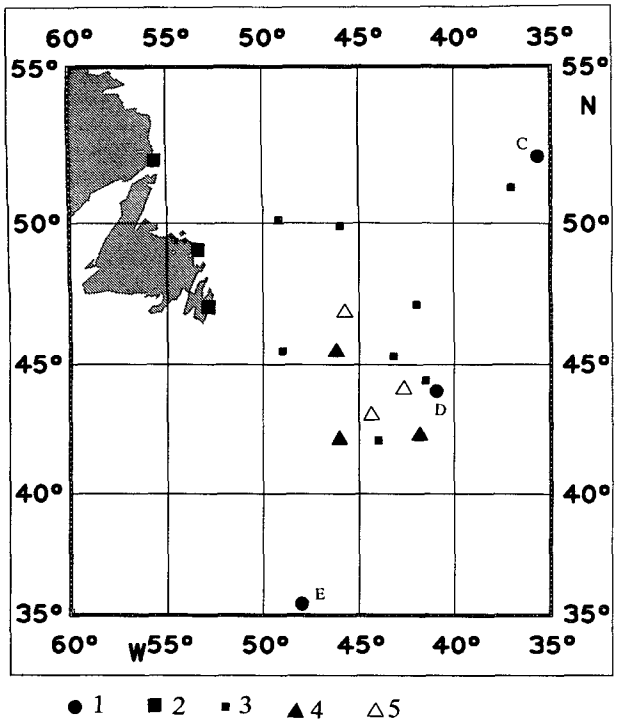

FIG. 1. Spatial distribution of meteorological datasets: 1—Ocean Weather Stations, 2—coastal meteorological stations, 3—meteorological buoys and platforms, 4—research vessels of NEWFOUEX 88 experiment, and 5—research vessels of ATLANTEX 90 experiment.

from Canadian shore stations. The most significant data were obtained during the stationary mesoscale meteorological experiments in the period 1980–1990 under the program "SECTIONS." This dataset consists of 48 records of hourly observations. The record lengths varied from 10 days to 2.5 months.

The most interesting time series were obtained during the NEUFOUEX-88 (Lappo et al. 1989) and ATLANTEX-90 (Gulev et al. 1991) experiments. Both of these experiments, as well as the earlier experiment, NEWFOUEX-84, were designed to study air–sea interaction processes in Newfoundland Basin during the periods from November 1987 to April 1988 and from December 1989 to May 1990, respectively. Ships, balloons, buoys, and moorings were used to measure the atmospheric and oceanic structures and properties. Although the measurement program was designed primarily for the region 40°–48°N, 40°–48°W, this study includes all voluntary meteorological observations that were onboard each of five research vessels during hydrological surveys (four surveys for each experiment) and during the stationary phases of the experiments (22 days in March 1988 and 24 days in April 1990, respectively), when three vessels situated in fixed positions (Fig. 1) and two others carried out surveys in the vicinity of the triangles. Fortunately during March 1988 and April 1990 the number of voluntary (primary fishery) ships in this region was relatively high. Additional hourly meteorological measurements were obtained from voluntary ships courtesy of radio contacts. Later (section 3, Table 1), more detailed information will be given about the spatial distribution of meteorological measurements. In total, more than 300 000 meteorological observations from ocean weather stations (approximately 32 000 hourly observations from stationary experiments and more than 120 000 voluntary meteorological observations) were used.

3. The bulk aerodynamic calculations under classical and sampling approaches

The bulk aerodynamic formulas for the sensible heat flux, Q_H; the latent heat flux, Q_E; and momentum flux, Q_V, were used in the following form:

$$Q_H = C_p \rho_a C_T V \delta T,$$

$$Q_E = L\rho_a \frac{0.622}{P} C_E V \delta e,$$

$$Q_V = \rho_a C_V V^2, \qquad (1)$$

where $\delta T = T_w - T_a$; $\delta e = e_0 - e_z$; T_w is water temperature; T_a is air temperature, e_z is water vapor pressure; e_o is saturation vapor pressure; connected with T_W, V is wind speed; ρ_a is air density; C_p is specific heat of air at constant pressure; L is the latent heat of evaporation of water; and C_T, C_E, and C_V are the transfer coefficients known as the Stanton number, the Dalton number, and the Schmitt number, respectively. These coefficients were determined using the Ariel et al. (1981) approach, which is based on Monin–Obukhov similarity theory. After Ariel et al. (1981) C_T, C_E, and C_V depend on wind speed and stability and vary from 0.9×10^{-3} to 2.1×10^{-3}. This approach is very comparable with the Liu et al. (1979) method used by Esbensen and Reynolds (1981). Figure 2 demonstrates the comparison of the Ariel et al. (1981) and Liu et al. (1979) schemes. For calculation of the Liu et al. (1979) coefficients, the FORTRAN program documented in Liu and Blanc (1984) has been used. The heat transfer coefficient used in this study is in good agreement with Liu et al. (1979) under moderate winds and is 10%–15% higher under relatively strong winds. The drag coefficient is 10% smaller than that in Liu et al. (1979) under moderate winds and very close to Liu et al. (1979) for $10 < V < 14$ m s^{-1}, if we use the Kondo (1975) scheme for a neutral drag coefficient in the Liu et al. (1979) parameterization. In the case of a combination of the Liu et al. (1979) with the Large and Pond (1981) schemes for a neutral drag coefficient, Ariel et al. (1981) gives 20% higher C_V for strong winds and very close to that of Liu et al. (1979) under calm and moderate winds. [One can find (Fig. 2) from 10% to 25% differences even between the two versions of the Liu et al. (1979) parameterization.] For storm con-

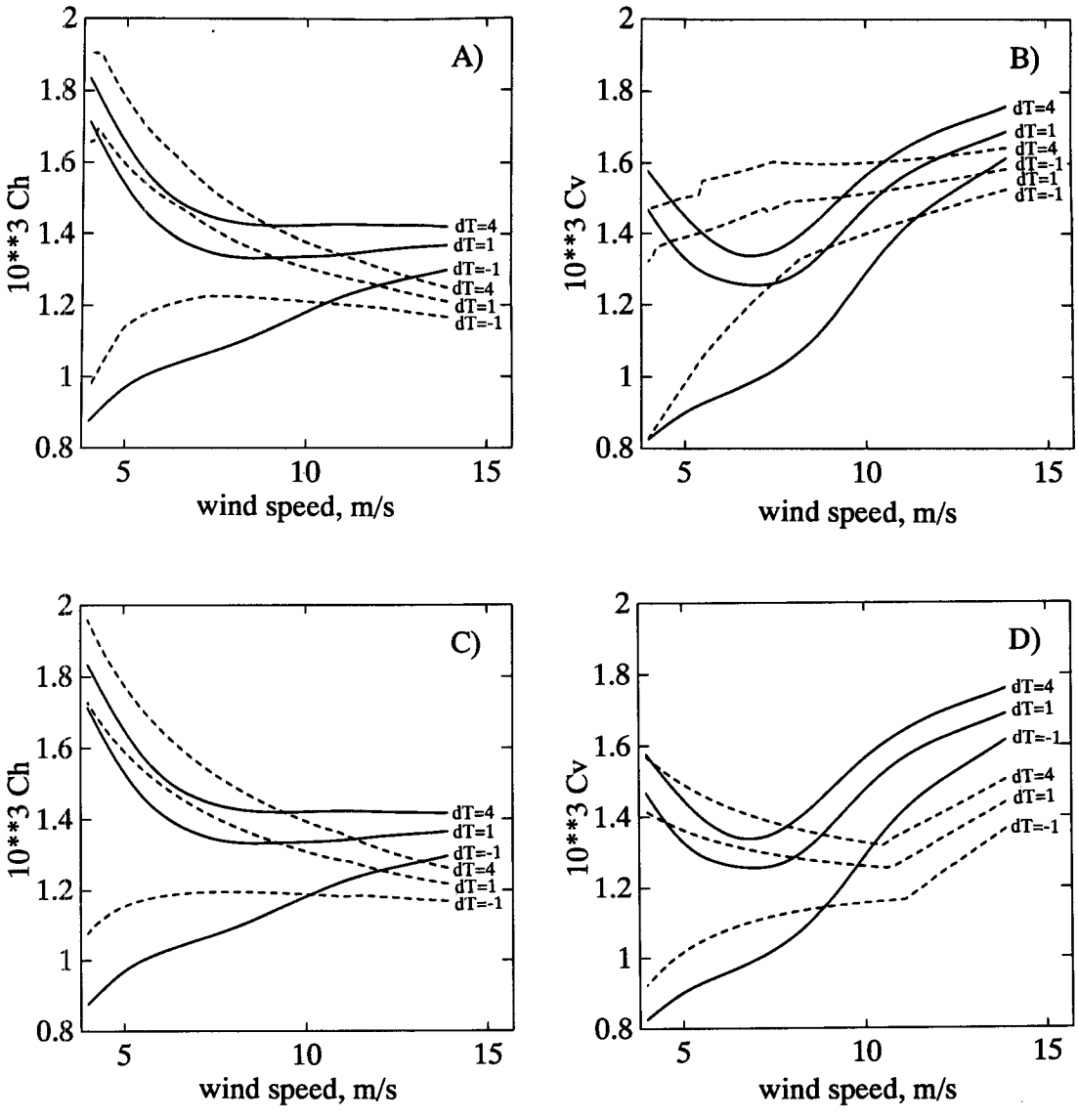

FIG. 2. Comparison of Ariel et al. (1981) (solid lines) and Liu et al. (1979) (dashed lines) schemes for heat transfer coefficient (a), (c) and drag coefficient (b), (d); (a), (b) the combination of Liu et al. (1979) scheme with Kondo (1975) scheme for neutral drag coefficient; (c), (d) the combination of Liu et al. (1979) scheme with Large and Pond (1981) scheme for neutral drag coefficient.

ditions ($V > 14$ m s^{-1}) the Bortkovskiy (1983) approximation was used. In the case when $V < 3$ m s^{-1} (less than 2% of observations) under free convection conditions, C_T and C_E coefficients were computed by the Grachov and Panin (1984) method.

When formulas (1) are used for individual values of meteorological parameters, it is easy to obtain averaged fluxes (the so-called sampling method). Alternatively, we can estimate averaged fluxes taking into consideration averaged meteorological parameters (the so-called classical method). The relationship between the two methods is given by

$$\begin{aligned}\langle C_T V \delta T\rangle_\tau &= \langle C_T\rangle_\tau\langle V\rangle_\tau\langle \delta T\rangle_\tau \\ &+ \langle C_T\rangle_\tau\langle V'\delta T'\rangle_\tau + \langle C'_T\delta T'\rangle_\tau\langle V\rangle_\tau \\ &+ \langle C'_T V'\rangle_\tau\langle \delta T\rangle_\tau + \langle C'_T V'\delta T'\rangle_\tau. \quad (2)\end{aligned}$$

This equation illustrates the dependence of fluxes on spatial- and temporal-averaging scales. This dependence occurs because of the correlation between the meteorological parameters and the nonlinearity of the bulk formulas (1). In (2) $\langle\ \ \rangle_\tau$ is the time-averaging operator. Similar equations can be written for space averaging ($\langle\ \ \rangle_r$), space–time averaging ($\langle\ \ \rangle_{\tau,r}$), and

for latent heat flux ($\langle C_E \delta e V \rangle$) and momentum flux ($\langle C_V V^2 \rangle$). In this study temporal averaging with time scale τ was given by the low-pass digital filtration of sample series $T(t)$:

$$\langle T \rangle_\tau(t_i) = \frac{1}{\tau} \int_{t_i-\tau/2}^{t_i+\tau/2} T(t)dt. \quad (3)$$

To examine the spatial averaging we choose 69 datasets where the duration varied from a minimum of 1 day to a maximum of 19 days. All these datasets contained very high spatial resolution observations (more than 36 simultaneous meteorological measurements in a circle within a radius of 100 km). The location and duration of these datasets are presented in Table 1. Most of the data were collected for cold seasons, primarily for those periods when special meteorological observations on research vessels were also available. To produce regular data around each grid point, measurements were interpolated on a circular network with a number of nodes on each concentric circumference connected with averaging radius extension, δr:

$$n_k = n_0(r_0 + k\delta r)/r_0,$$

where k is the number of extensions, r_0 the initial radius, and n_0 the initial number of nodes. This network was adjusted to equalize the grid point separation in r and ϑ, where ϑ is polar angle. Figure 3 demonstrates an example of the location of nodes for $r_0 = \delta r = 40$ km. The spatial average for every grid point was then given by

$$\langle T \rangle_r = \frac{1}{\pi r^2} \int_0^R \int_0^\theta T(r, \vartheta) r d\vartheta dr. \quad (4)$$

In this study we consider a wide range of temporal- and spatial-averaging scales. The estimates were obtained for sampling periods (τ) of 1, 3, 6, 12 h; 1, 2, 3, 5, 7.5, 10 d; 1, 3, 6 mo; and 1, 2, 10, 20 yr. For spatial averaging the diameter ($d = 2r$) varied from a minimum of 40 km to a maximum of 800 km. For time scales of less than 10 days, the joint effects of spatial and temporal averaging were considered.

According to (2) the following coefficients were used to describe the influence of the averaging on heat and momentum flux estimates:

TABLE 1. Location and duration of datasets used for examination of spatial averaging.

N	Latitude (North)	Longitude (West)	Duration	Number of observations	N	Latitude (North)	Longitude (West)	Duration	Number of observations
1	38°-44.5°	42°-45°	28-31 Oct 82	681	36	43.5°-48°	54°-62°	11-23 Aug 87	5731
2	43°-49°	51.5°-64°	5-6 Nov 82	104	37	38°-40.5°	50°-53°	26-29 Nov 87	529
3	46°-53°	41°-45°	21-24 Dec 82	328	38	46°-53°	41°-46.5°	5-8 Feb 88	438
4	44°-48°	46°-50.5°	23-26 Sep 83	711	39	40°-42°	47.5°-50°	10 Feb 88	96
5	47.5°-56°	50°-54°	11-12 Oct 83	293	40	37°-40°	52°-58°	11 Feb 88	124
6	37°-41°	45°-50°	23-30 Dec 83	1386	41	46°-53°	35.5°-39°	11 Feb 88	69
7	46.5°-48.5°	41°-43°	24 Dec 83	24	42	38°-44°	56°-61°	7-13 Feb 88	1070
8	37.5°-41°	40°-47.5°	4-16 Jan 84	4132	43	41°-46°	39.5°-43.5°	18-21 Feb 88	1237
9	48°-51°	47.5°-50°	8-10 Jan 84	131	44	41.5°-46.5°	41°-47.5°	3-21 Feb 88	6134
10	43°-46°	40°-42.5°	18 Jan 84	91	45	46°-54°	51°-56°	9-14 Feb 88	1382
11	41°-44°	43°-46°	19-20 Jan 84	106	46	38°-43°	39°-40.5°	12-16 Mar 88	316
12	38°-40°	48.5°-52°	21-22 Dec 84	86	47	51°-54°	35°-42°	7-10 Mar 88	761
13	39°-43.5°	42°-45.5°	24 Jan-22 Dec 84	1069	48	40°-47.5°	38.5°-52°	22 Mar 88	298
14	47°-52°	42°-46°	9-14 Feb 84	311	49	50°-53°	46°-49°	24 Mar 88	86
15	52°-54°	35°-38°	17 Feb 84	80	50	40°-44°	49.5°-55°	29.3-2 Apr 88	171
16	47°-49°	36.5°-38.5°	18 Feb 84	57	51	37°-41°	36°-40°	1-6 Apr 88	621
17	44°-49°	47.5°-52.5°	17-20 Feb 84	219	52	41°-45°	54°-60°	21.5-2 Jun 88	1629
18	36.5°-43°	41°-49°	28-29 Feb 84	369	53	50.5°-54.5°	45°-52°	24-25 May 88	731
19	39°-46°	45°-52°	23 Nov-6 Dec 84	3874	54	38°-46°	57°-62°	15-19 Aug 88	828
20	47°-51°	39°-44°	17-19 Jan 85	184	55	42°-47°	53°-58°	2-9 Nov 88	1056
21	36°-42°	51°-57°	26 Jan 85	172	56	44°-49.5°	40°-44.5°	4-9 Nov 88	794
22	46°-49°	41°-44°	29 May-4 Jun 85	172	57	46°-53°	39°-46°	15-23 Mar 89	2031
23	44°-49°	49°-55°	23 Jun-8 Jul 85	1717	58	38.5°-43°	56°-59.5°	6-18 Apr 89	1416
24	44°-48°	41.5°-45.5°	14-15 Jul 85	93	59	43°-48°	50°-57°	24-26 Jul 89	917
25	46°-50°	50°-52.5°	2 Sep 85	51	60	44°-46°	42°-44°	28 Jul 89	161
26	39°-45°	43°-51°	14-20 Oct 85	1151	61	45°-48°	38°-41°	29 Jul 89	147
27	45°-50°	40°-45°	23-26 Oct 85	108	62	39°-49°	53°-61°	9-15 Oct 89	2089
28	41°-46°	43°-51°	4-12 Nov 85	819	63	46°-50.5°	49°-54°	4-14 Mar 90	1241
29	47.5°-51.5°	35°-38.5°	15-17 Nov 85	334	64	42°-47°	39°-44°	8-13 Mar 90	738
30	38°-42°	36.5°-40°	21 Nov 85	46	65	46°-50°	40.5°-46°	20-26 Mar 90	591
31	44°-47.5°	45°-51°	3-10 Mar 86	4934	66	41°-49.5°	42.5°-48°	4-20 Apr 90	5378
32	39°-42°	47°-63°	16-21 Jun 86	3721	67	47.5°-51.5°	40°-52°	29.4-11 May 90	1098
33	45°-52°	41°-47°	9-12 Oct 86	1223	68	49°-55°	44°-48°	5-12 Oct 90	488
34	51°-54.5°	38°-43°	12-18 Mar 87	938	69	47.5°-53°	43°-47°	16-20 Nov 90	794
35	49°-53°	40.5°-44°	21-22 Mar 87	431					

$$\xi_H(\tau) = \frac{\langle C_T V \delta T \rangle_\tau}{\langle C_T \rangle_\tau \langle V \rangle_\tau \langle \delta T \rangle_\tau},$$

$$\xi_E(\tau) = \frac{\langle C_E V \delta e \rangle_\tau}{\langle C_E \rangle_\tau \langle V \rangle_\tau \langle \delta e \rangle_\tau},$$

$$\xi_V(\tau) = \frac{\langle C_V V^2 \rangle_\tau}{\langle C_V \rangle_\tau \langle V \rangle_\tau^2}. \quad (5)$$

The same coefficients can be written for spatial [$\xi(r)$] and for space–time averaging [$\xi(\tau, r)$]. Since the denominator of ξ_H can go to zero, we assumed $\delta T = \delta T + 0.05$ for $\delta T = 0$ to exclude near-neutral values from the empirical determination of ξ_H. For a number of years there was considerable debate as to the proper method of wind speed averaging in order to choose between scalar and vector averaging (Saunders 1976; Wright and Thompson 1983; Thompson et al. 1983; Marsden and Pond 1983; Hanava and Toba 1987; Lander et al. 1989; Weare 1989). The most comprehensive studies were made by Hanava and Toba (1987) and Thompson et al. (1983), the latter proposed a formalism that gives good agreement with Willebrand's (1978) results. Most authors found differences between scalar and vector averaging that are significant for wind stress component calculations. However, we will discuss in this study scalar averaging, which is used more often for heat and moisture flux estimates (Kondo 1972; Fissel et al. 1977; Esbensen and Reynolds 1981; Simmonds and Dix 1989).

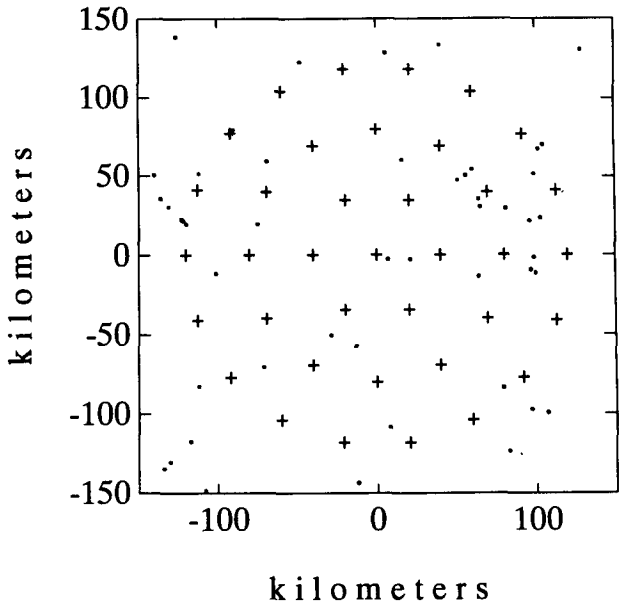

FIG. 3. Example of the location of nodes of the circular network (crosses) and spatial distribution of voluntary observations (dots) for 13 February 1988.

4. The results

a. Temporal averaging

The time-averaging influence on the flux estimates is shown in Fig. 4 for all periods. The coefficients (5) for fixed-averaging periods are given in Table 2. For averaging periods less than one month, sensible and latent heat fluxes decrease by 43% and 47%, respectively. The most visible reduction of average estimates for both sensible and latent fluxes corresponds to the range $10 < \tau < 30$ days. Momentum flux estimates for the averaging period of 1 month are 1.5 times smaller in comparison with sampled observations. Generally, the most significant influence of temporal averaging on sensible and latent heat fluxes appears for the averaging periods from 10 days to 3 months. For momentum flux, the synoptic scales ($1 < \tau < 240$ h) give the most important contribution to the mean estimates. Our results demonstrate more significant differences between the classical and sampling methods than were obtained by Esbensen and Reynolds (1981) and Simmonds and Dix (1989). Esbensen and Reynolds (1981) deals with data for the period from 1948 until 1971–1972. This disagreement may be related to the long-term variability of intramonthly statistical properties of meteorological parameters and their monthly mean values over the North Atlantic. Previous calculations of intramonthly statistics (Gulev 1994) clearly show an increase in intramonthly mean square deviations of δT and δe in the period of 1975–1988 at least for OWS C. Besides, there are indications of a positive trend of monthly mean wind speed for the same period, obtained on the basis of Comprehensive Ocean–Atmosphere Dataset (COADS) data (Ramage 1984; Cardone et al. 1990; Lindau et al. 1990) and OWS data as well (Isemer and Lindau 1992; Isemer 1993). The point of discussion now is only about the reason for the observed trend, which may be caused by the use of inadequate Beaufort scales and different types of ships for different periods (Peterson and Hasse 1987; Isemer and Hasse 1991; Isemer 1993). We repeated our calculations for the period 1953–1972 to exclude the possible influence of the latest data. Coefficients ξ_H, ξ_E, and ξ_V for $\tau = 1$ month equaled 1.38, 1.19, and 1.40, respectively, which is less than presented in Table 2, but also higher in comparison with Esbensen and Reynolds (1981). Marsden and Pond (1983), using practically the same dataset as Esbensen and Reynolds (1981) and transfer coefficients after Pond et al. (1974) and Large and Pond (1981, 1982), obtained much clearer differences between the sampling and classical methods than Esbensen and Reynolds (1981). In contrast, Kondo (1972) obtained results similar to those of Esbensen and Reynolds (1981), using, however, only data from the year of 1959.

Another possible reason for the disagreement with Esbensen and Reynolds (1981) is the location of our dataset, which is mostly in the northwest Atlantic and characterized by strong synoptic and mesoscale vari-

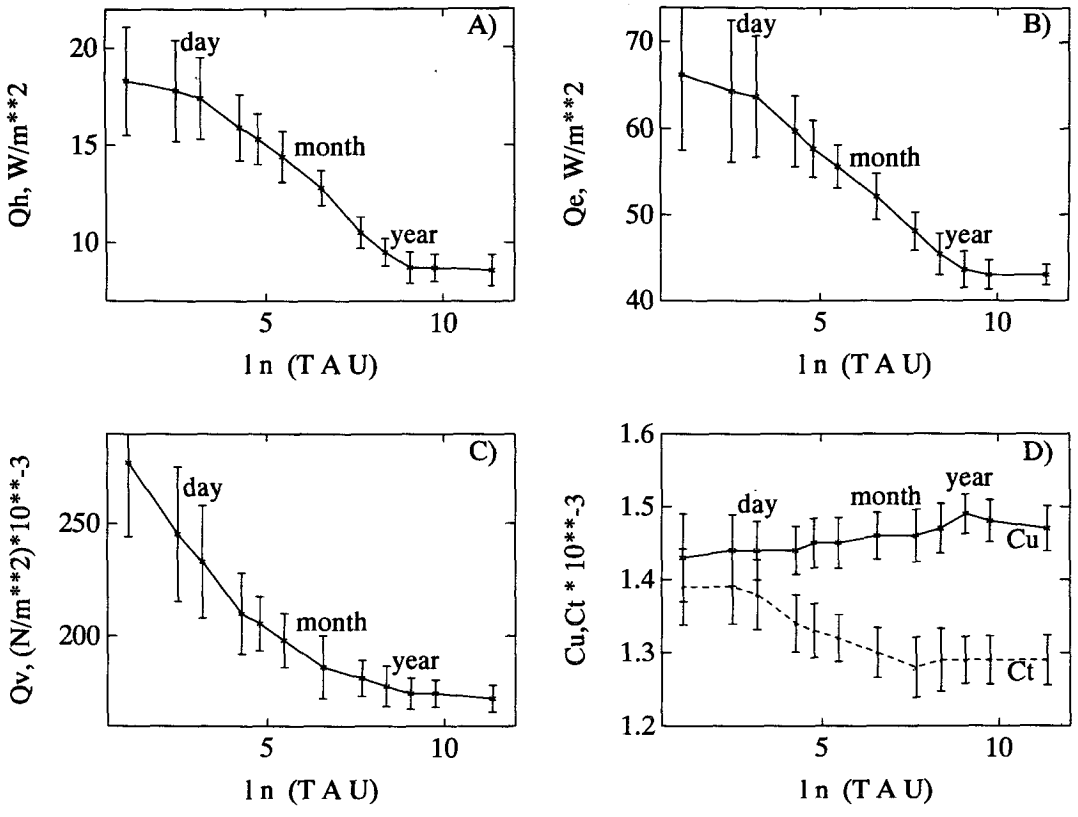

FIG. 4. The behavior of (a) sensible heat flux (W m^{-2}), (b) latent heat flux (W m^{-2}), (c) momentum flux (10^3 N m^{-1}), and (d) transfer coefficients C_T and $C_u(2)$ as a function of temporal-averaging scale.

ability of meteorological characteristics. According to Marsden and Pond (1983), OWS D has the largest difference between sampling and classical methods. However, Esbensen and Reynolds (1981) demonstrated good coincidence of both methods for OWS D. Further analysis of the differences in parameterizations of transfer coefficients used by Esbensen and Reynolds (1981), Marsden and Pond (1983), and present study can be continued in terms of different correlation terms of (2) (see Appendix); this is summarized in Fig. 4d, which demonstrates a weak dependence of transfer coefficients on averaging scale. The estimates shown here are more comparable with the Marsden and Pond (1983) calculations. Our results for sensible heat fluxes with synoptic averaging practically coincide with the results of Efimov et al. (1985), who obtained (for the Black Sea) ξ_H ranging between 1.2 and 1.3 for $\tau = 1$ mo and ξ_H ranging between 1.5 and 2.0 for $\tau = 1$ yr.

As shown in Fig. 5 the coefficients ξ_H, ξ_E, and ξ_V have a clear seasonal dependence. The coefficient ξ_H for $\tau = 1$ month varies from a minimum of 1.2 to 1.3 in winter to a maximum of 1.5 to 1.6 in spring and autumn. An absolute minimum is observed in July. However, the sensible heat fluxes for this month are close to zero and $\xi_H = 1.5$ in absolute form corresponds to $C_p\rho_a(\langle C_T V \delta T\rangle - \langle C_T\rangle\langle V\rangle\langle\delta T\rangle) = 0.5$ to 5.0 W m^{-2}, which is less than the accuracy of bulk calculations. Generally, as shown in Fig. 5, a significant seasonal march of ξ_H, ξ_E, ξ_V appears only for $\tau > 3$ days. For averaging scales less than 3 days the coefficients ξ_H, ξ_E, ξ_V can be assumed constant for all seasons.

To describe the behavior of the coefficients ξ_H, ξ_E, ξ_V on time-averaging scales, simple formulas were constructed. All the coefficients were considered as functions of wind speed and sea–air temperature differences for all averaging periods. It was assumed a priori that an appropriate general formula for ξ_H, ξ_E, ξ_V is the following:

$$\begin{Bmatrix} \xi_H \\ \xi_E \\ \xi_V \end{Bmatrix} = a_1(\ln\tau - a_2)\begin{Bmatrix} F_H \\ F_E \\ F_V \end{Bmatrix} + a_3, \qquad (6)$$

where τ is the averaging period in hours; a_1, a_2, and a_3, are empirical coefficients; F_H, F_E, and F_V are functions of sea–air temperature difference and wind speed. These functions describe the dependence of ξ_H, ξ_E, and ξ_V on dynamical conditions and stability, which is presented in Fig. 6 for ξ_H and ξ_E for $\tau = 1$ mo. Coefficient ξ_H decreases with both sea–air temperature differences and wind speed. The behavior of ξ_V with wind speed is similar. In contrast with ξ_H and ξ_V, the coefficient ξ_E

TABLE 2. Coefficients (5) dependence on time-averaging scales.

	Sampled observations	Hours						Months				
		6	12	24	72	120	240	1	3	6	12	24
ξ_H	1.00	1.02	1.03	1.05	1.15	1.20	1.27	1.43	1.75	1.93	2.10	2.10
ξ_E	1.00	1.01	1.03	1.04	1.11	1.15	1.19	1.27	1.38	1.46	1.52	1.54
ξ_V	1.00	1.08	1.13	1.19	1.32	1.35	1.40	1.49	1.53	1.56	1.59	1.59

increases with δ_e and V. This is the reason for differences in annual cycle between ξ_H and ξ_V coefficients on one hand and ξ_E on the other (Fig. 5). Thus, functions F_H, F_E, and F_V in general form were written as

$$F_H = 1 + 1/(\alpha|\langle \delta T\rangle| + \beta\langle V\rangle),$$
$$F_E = 1 + \alpha\langle \delta T\rangle + \beta\langle V\rangle,$$
$$F_V = 1 + 1/\beta\langle V\rangle, \qquad (7)$$

where the angular brackets indicate averaging over a fixed period. The parameters a_1, a_2, a_3, α, and β were chosen to minimize the mean square errors in formulas (6), (7). Actually coefficients a_1, a_2, and a_3 were firstly determined for constant F, corresponding to mean values of δT, δe, and V. After that α and β were calculated for fixed a_1, a_2, and a_3. All the parameters were determined for two ranges of time-averaging scales that correspond to intramonthly and intermonthly averaging. For the difference stability conditions ($\delta T > 0$, $\delta T < 0$) different parameters were also determined. All parameters in (6) and (7) for different ranges of averaging periods and stability conditions are given in Tables 3 and 4. Marsden and Pond (1983) also determined the power law behavior with wind speed of the coefficients of the kind in (5). Their formula includes three empirical coefficients. They also demonstrate the decrease of ξ_H and ξ_V with wind speed. However, in contrast to our study, Marsden and Pond (1983) found a negative power law for ξ_E. The principal difference is that Marsden and Pond (1983) used the vector-averaged wind speed in their empirical formula. Using for a very rough estimate the relation between mean scalar wind speed and mean vector wind speed of Thompson et al. (1983), we found reasonable agreement between (6) and the formulas of Marsden and Pond (1983), at least for sensible and momentum fluxes.

b. Spatial averaging

We now turn our attention to spatial averaging. As before we have calculated the coefficient (5) for fixed space-averaging scales (Table 5) and the behavior of sensible heat, latent heat, and momentum fluxes with an increase of the averaging diameter (Fig. 7). Since Fig. 7 indicates two definite breaks in the slope at $d = 2r$

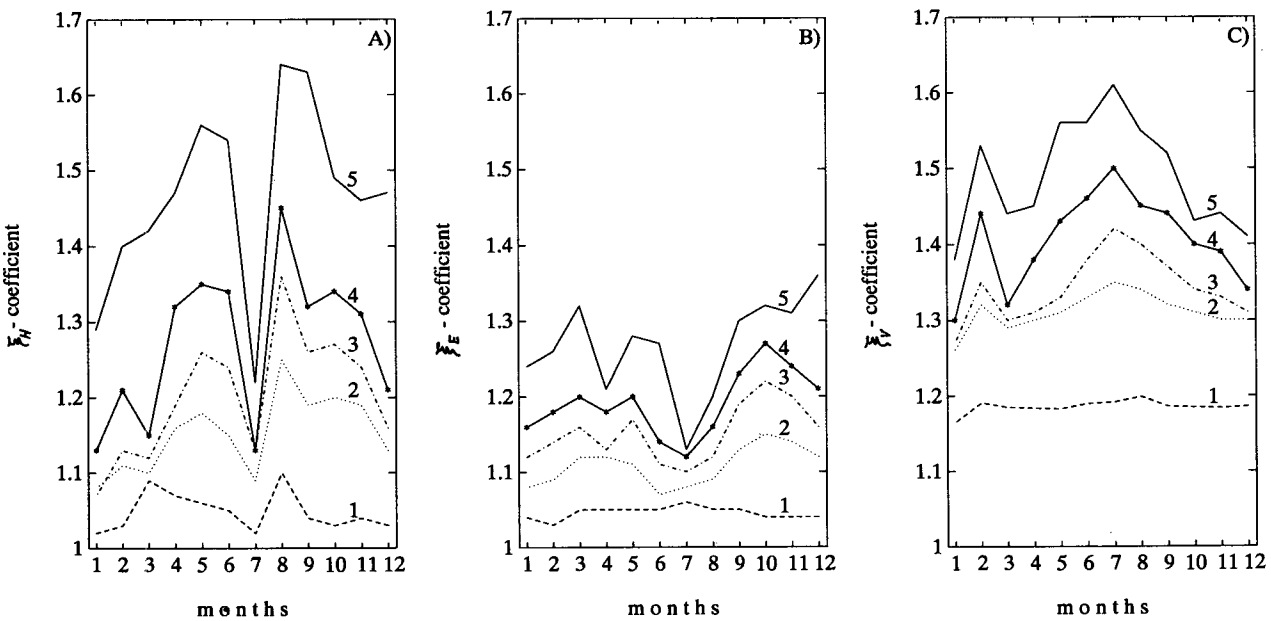

FIG. 5. Seasonal dependence of the coefficients ξ_H (a), ξ_E (b), and ξ_V (c) for different scales of temporal averaging: 1–24 h, 2–72 h, 3–120 h, 4–240 h, 5–720 h.

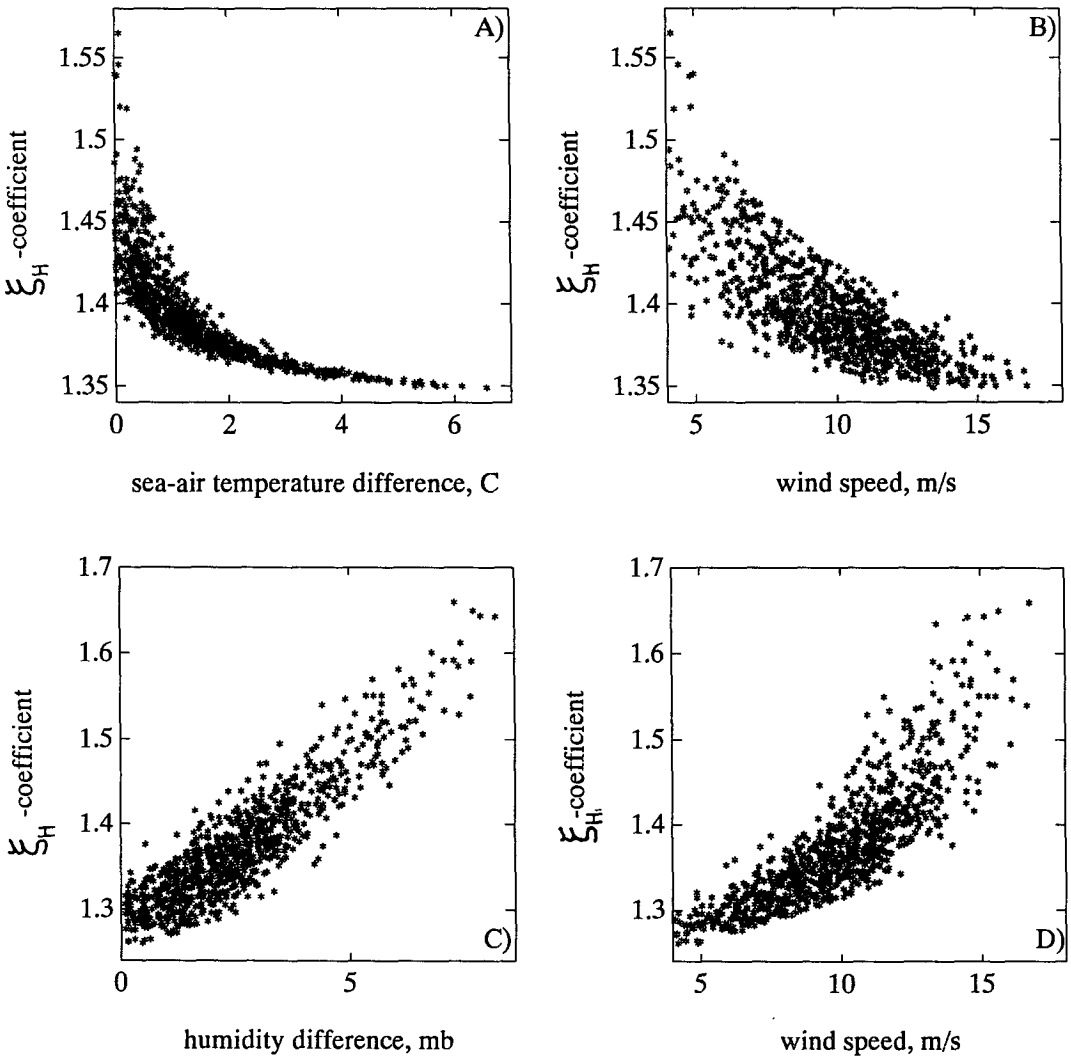

FIG. 6. The dependence of $\xi_H(\tau)$ (a), (b) and $\xi_E(\tau)$ (c), (d) coefficients on stability (a), (c) and wind speed (b), (d).

$\approx$ 280 km and $d = 2r \approx 560$ km, three ranges are manifested in the behavior of energy fluxes. The first range (0–320 km) is characterized by exponential decreases of the fluxes. In the second range (320–560 km), linear 7%–10% decreases of Q_H and Q_E appear. The third range (560–800 km) is characterized by a nonlinear 20%–25% reduction of fluxes. Unlike for temporal averaging, ξ_E values are greater than ξ_H, so spatial averaging is more significant for latent heat flux than for sensible heat flux. The momentum flux dependence on spatial-

TABLE 3. The a_1, a_2, and a_3 values for the formulas (6) for different ranges of time-averaging periods.

	Range 1 (24–720 h)			Range 2 (2–24 mo)		
	a_1	a_2	a_3	a_1	a_2	a_3
ξ_H, $\delta T > 0$	0.096	2.941	0.980	0.089	2.636	1.076
ξ_H, $\delta T < 0$	0.107	2.317	1.041			
ξ_E	0.052	3.144	1.039	0.063	3.826	1.023
ξ_V	0.094	2.291	1.021	0.102	0.841	1.058

TABLE 4. The α and β values for formulas (7) for different ranges of time-averaging periods.

	Range 1 (24–720 h)		Range 2 (2–24 mo)	
	α	β	α	β
F_H, $\delta T > 0$	2.847	0.552	3.146	0.271
F_H, $\delta T < 0$	2.114	0.761		
F_E	0.059	0.034	0.109	0.084
F_V		1.289		0.542

TABLE 5. Coefficients (5) dependence on space-averaging scales.

	Sampled observations	Kilometers									
		80	160	240	320	400	480	560	640	720	800
ξ_H	1.00	1.09	1.19	1.26	1.28	1.31	1.33	1.35	1.40	1.50	1.69
ξ_E	1.00	1.11	1.19	1.28	1.34	1.38	1.42	1.46	1.52	1.63	1.81
ξ_V	1.00	1.02	1.06	1.23	1.31	1.26	1.21	1.18	1.27	1.44	1.55

averaging scales is not monotonic. In the range $280 < 2r < 560$ km, momentum flux increases about 15% percent with the spatial-averaging scale. This can be associated with very strong differences between wind speed estimates in different parts of midlatitude cyclones. Consequently, in the range of averaging scales from 280 to 560 km, mesoscale meteorological features are already averaged, but the statistics of separate parts of atmospheric cyclones are still detectable. Anyway, this fact can be one of the reasons for Q_V increasing in the range of $280 < 2r < 560$ km.

To construct approximate formulas for the coefficients $\xi_H(r)$, $\xi_E(r)$, and $\xi_V(r)$, stability and dynamical conditions were taken into consideration. Figure 8 demonstrates the dependence of ξ_H and ξ_E on δT and δe for the spatial-averaging diameter equal to 560 km. Estimates show that the influence of spatial averaging on sensible heat flux decreases with increasing δT and increases with the wind speed. For the latent heat flux δe and increasing wind speed, $\xi_E(1)$ increases, although the correlation with wind speed is much higher than with δe. When spatial-averaging scales are more than 600 km, the coefficients of $\xi_H(r)$, $\xi_E(r)$, and $\xi_V(r)$ appear to be practically independent of stability and determined by wind speed only. Finally the following formulas were constructed:

$$\begin{Bmatrix} \xi_H \\ \xi_E \end{Bmatrix} = \begin{cases} b_1(\ln(2r) - b_2)|\langle \delta T \rangle|^{\gamma} V^{\lambda} + b_3, \\ \qquad 0 < 2r < 280 \text{ km} \\ c_1 2r + c_2\langle \delta T \rangle + c_3\langle V \rangle + c_4, \\ \qquad 280 < 2r < 560 \text{ km} \\ \exp[d_1(2r - d_2)]\langle V \rangle^{\varphi}, \\ \qquad 560 < 2r < 800 \text{ km} \end{cases} \tag{8}$$

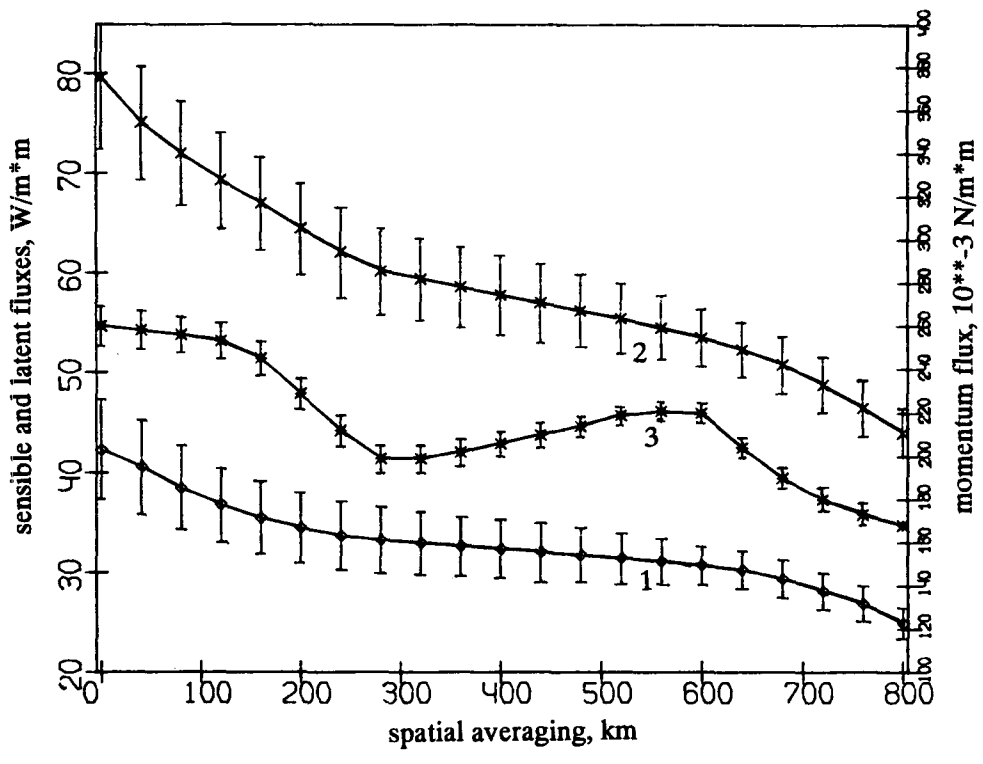

FIG. 7. The behavior of sensible heat flux (1), latent heat flux (2), and momentum flux (3) in dependence of spatial-averaging scale.

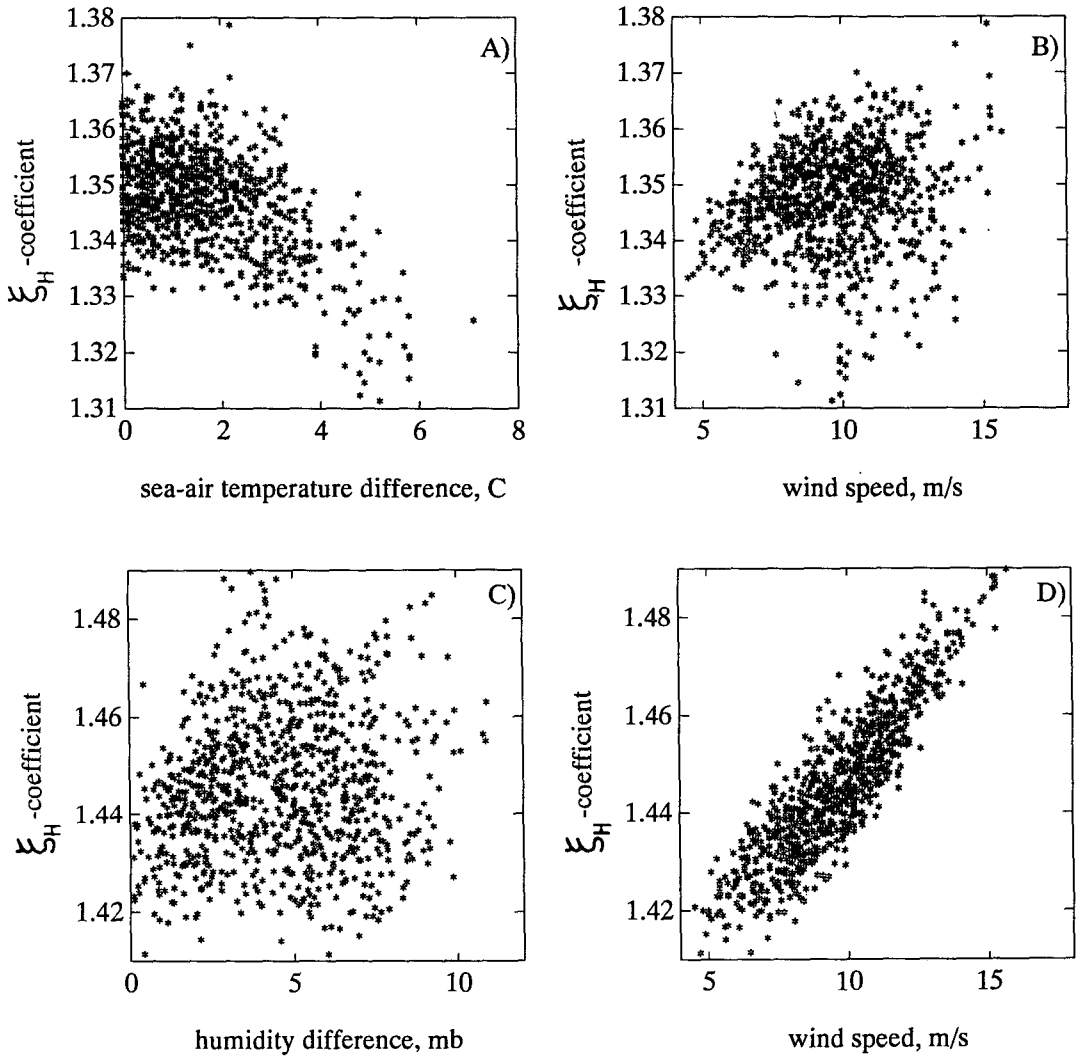

FIG. 8. The same as in Fig. 6 but for spatial coefficients $\xi_H(r)$ (a), (b) and $\xi_E(r)$ (c), (d).

$$\xi_V = \begin{cases} \exp[1.0276 \times 10^{-3} \cdot 2r]\langle V \rangle^{0.063}, & 0 < 2r < 280 \text{ km} \\ -0.589 \times 10^{-3} \cdot 2r - 0.0051\langle V \rangle + 1.546, & 280 < 2r < 560 \text{ km} \\ 0.954[\ln(2r) - 6.304]\langle V \rangle^{0.020} + 1.149, & 560 < 2r < 800 \text{ km}, \end{cases} \quad (9)$$

where as before angular brackets indicate spatial averaging over the area with fixed-averaging radius; $2r$ is averaging diameter in kilometers; and b_i, c_i, d_i, γ, λ, and φ are empirical coefficients that were chosen the same way as (6) and (7). We constructed approximate formulas for ξ_H and ξ_E separately for different ranges, using logarithmic (0–280 km), linear (280–560 km), and exponential (560–800 km) functions. The reasons are definite breaks in Fig. 7 and considerable decreases in δT and δe influence on ξ_H and ξ_E for $V > 560$ km. The mean square errors obtained for these multirange approximations (see section 5) are much less than in the case of the use of universal functions for all the range of 0–800 km. To examine this choice, polynomial-logarithmic and polynomial-trigonometric functions were also used. These coefficients for the different ranges of averaging scales and for the different stability conditions are given in Table 6. Mahrt (1987) obtained a relationship between heat transfer coefficient for area-averaged fluxes over the land and the transfer coefficient at neutral stability, taken from sampled observations according to the Louis (1979) parameterization. His formula indicates an exponential law with Richardson number, which appears to be a function of stability. However, his formulation includes the joint effect of

TABLE 6. The b_i, c_i, d_i, γ, λ, and φ values for the formulas (8) for different ranges of space-averaging scales.

	$\xi_H(r)$		
	$\delta T > 0$	$\delta T > 0$	$\xi_E(r)$
b_1	0.107	0.114	0.104
b_2	3.221	2.964	2.886
b_3	1.031	1.014	1.014
c_1	2.947×10^{-4}	2.521×10^{-4}	4.683×10^{-4}
c_2	−0.0089	−0.0104	0.0024
c_3	0.0046	0.0059	0.0071
c_4	1.184	1.207	1.153
d_1	0.7931×10^{-3}	0.7931×10^{-3}	0.8404×10^{-3}
d_2	256.3	256.3	226.2
γ	−0.107	−0.094	0.054
λ	0.029	0.018	0.038
φ	0.036	0.036	0.059

turbulent processes in the sampling case and averaging. Thus, there is no possibility to consider separately averaging effects outside the framework of Louis's (1979) parameterization.

Thus, taking into account (6), (7), (8), and (9), we can calculate the contribution of spatial- and temporal-averaging effects to the estimates of sensible heat, latent heat, and momentum fluxes. Consequently, for the use of averaged parameters, formulas (1) can be rewritten in the following form:

$$Q_H = C_p \rho_a C_T(\langle V \rangle, \langle \delta T \rangle) \begin{Bmatrix} \xi_H(\tau) \\ \xi_H(r) \end{Bmatrix} \langle V \rangle \langle \delta T \rangle,$$

$$Q_E = L\rho_a \frac{0.622}{P} C_E(\langle V \rangle, \langle \delta T \rangle) \begin{Bmatrix} \xi_E(\tau) \\ \xi_E(r) \end{Bmatrix} \langle V \rangle \langle \delta e \rangle,$$

$$Q_V = \rho_a C_V(\langle V \rangle, \langle \delta T \rangle) \begin{Bmatrix} \xi_V(\tau) \\ \xi_V(r) \end{Bmatrix} \langle V \rangle^2, \qquad (10)$$

which contain the ξ_H, ξ_E, and ξ_V coefficients.

c. *Joint spatial and temporal effects*

Actual climatological estimates of energy exchange between the ocean and the atmosphere are based on the space–time averaging of datasets. Hence it is necessary to take into consideration joint effects of spatial averaging and temporal averaging. The datasets of the NEWFOUEX-84, NEWFOUEX-88, and ATLANTEX-90 experiments were used to study joint effects of temporal and spatial averaging. These datasets contain both hourly meteorological measurements at stationary points during the periods, varying from a minimum of 13 days to a maximum of 19 days, and meteorological observations of the research vessels, voluntary ships, and fishery ships around these stationary points. The distances between stationary points (three for every experiment) varied in the range of 150 to 250 miles. As mentioned before, the spatial resolution of the synchronic spatial data corresponded to the condition $N(r = 100) > 36$. The details of these experiments were described by Gulev and Kolinko (1987), Lappo et al. (1989), Gulev and Kolinko (1990), and Gulev et al. (1991). Three datasets for the November 1984, March 1988, and April 1990 (the numbers 7, 44, and 66 in Table 1) experiments were prepared.

First of all it is interesting to determine the relationship between spatial-averaging scales and temporal-averaging scales for ocean–atmosphere exchange processes. To do this, values of $\xi_H(r)$, $\xi_E(r)$, and $\xi_V(r)$ were calculated step-by-step for every fixed $\xi_H(\tau)$, $\xi_E(\tau)$, and $\xi_V(\tau)$, respectively, with the purpose to find those averaging radii for which

$$\xi_H(\tau) = \xi_H(2r), \quad \xi_E(\tau) = \xi_E(2r), \quad \xi_V(\tau) = \xi_V(2r). \qquad (11)$$

For every averaging period (here we used higher resolution in τ than in section 2a) from 6 to 39 estimates of r were obtained. Figure 9 demonstrates the results in the form of curves, corresponding to the conditions (11) for sensible and latent fluxes. For momentum flux, due to the nonmonotonic behavior of $\xi_V(r)$, it is impossible to find simple correspondence between τ and r at least for $0 < 2r < 560$ km. Nevertheless, for both sensible and latent fluxes, one can find a relationship between spatial- and temporal-averaging scales. In terms of differences between sampling and classical estimates, temporal averaging within $\tau = 120$ h leads to the same results, as spatial averaging within 160 km for sensible heat flux and within 100 km for latent heat flux. Spatial averaging on scales of more than 200 km is comparable to temporal averaging within $\tau = 8$–12 days. Figure 9 shows that the $\tau(r)$ dependence appears to be different for sensible heat and for latent heat. This could be taken into account for the construction of boundary conditions for circulation models. The relatively large error bars in Fig. 9 prohibit serious consideration of analytical approximation for the explored relationships. Nevertheless, we give simple formulas, which were derived to approximate the dependence $\tau(2r)$ for the sensible heat fluxes and latent heat fluxes:

$$\tau_H = -1.5182 \times 10^4 (2r)_H^{-0.961} + 267.4,$$

$$\tau_E = -0.8842 \times 10^4 (2r)_E^{-0.987} + 261.7, \qquad (12)$$

for τ in hours and r in kilometers. Since square errors of (12) appear to be from 50% to 120% of averaging period or radius, one must use these formulas very carefully for relatively rough estimates.

On the basis of the same datasets, coefficients (5) for space–time averaging $[\xi(\tau, r)]$ were calculated. All estimates have been produced for the different spatial scales, corresponding to the fixed-averaging periods. The results are shown in Fig. 10. Joint space–time av-

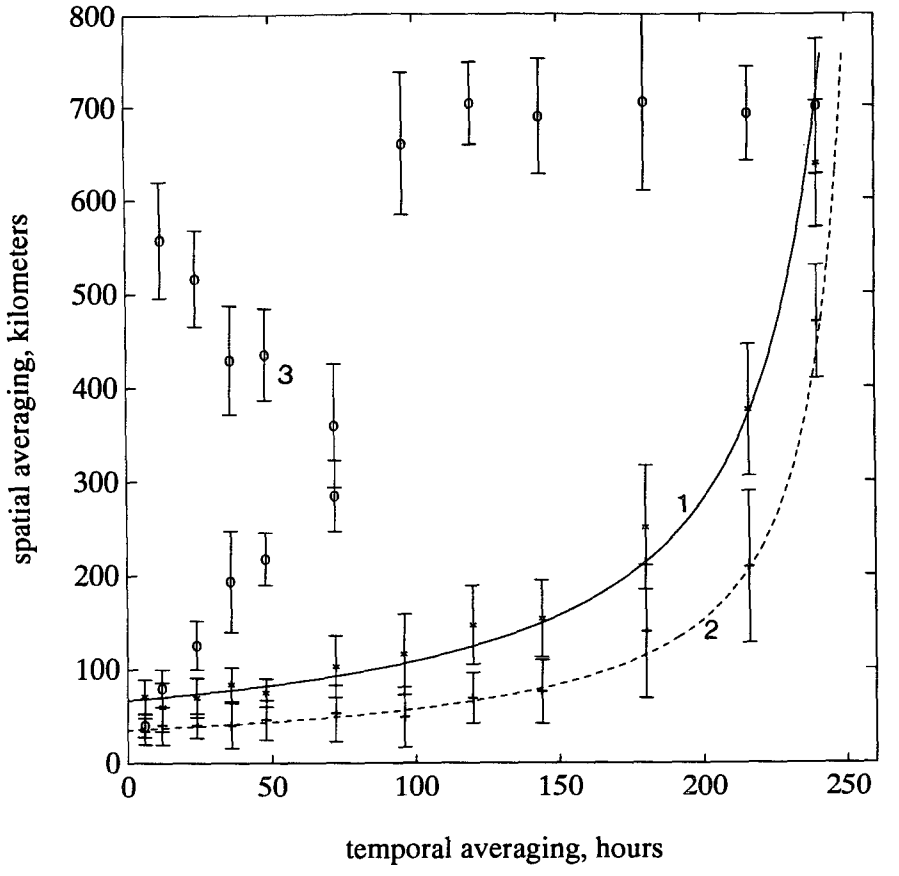

FIG. 9. Spatial- and temporal-averaging scales, for which $\xi_H(\tau) = \xi_H(r)$ (1), $\xi_E(\tau) = \xi_E(r)$ (2), $\xi_V(\tau) = \xi_V(r)$ (3).

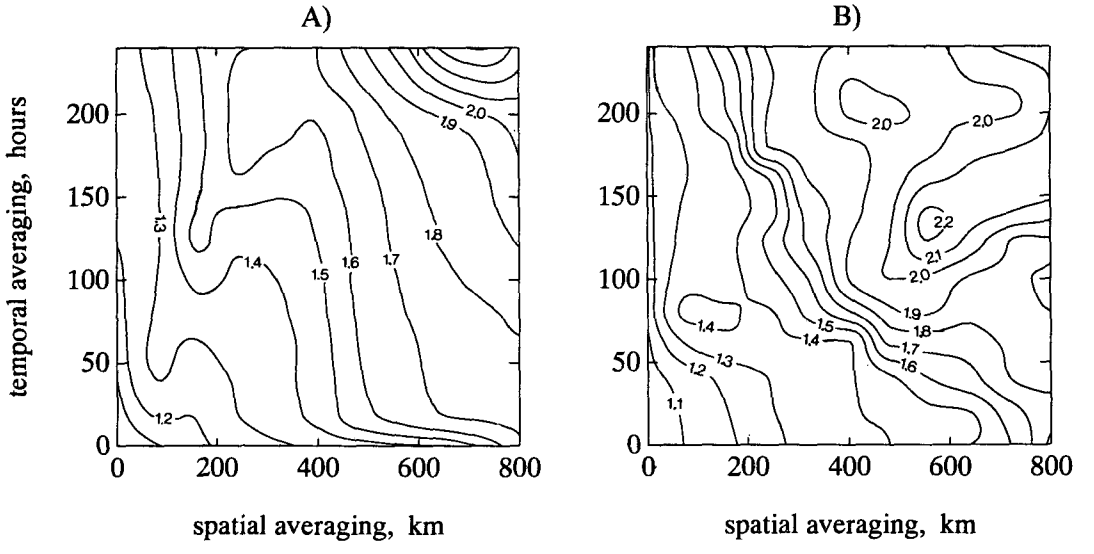

FIG. 10. The coefficients $\xi_H(\tau, r)$ (a) and $\xi_E(\tau, r)$ (b) as functions of temporal- and spatial-averaging scales.

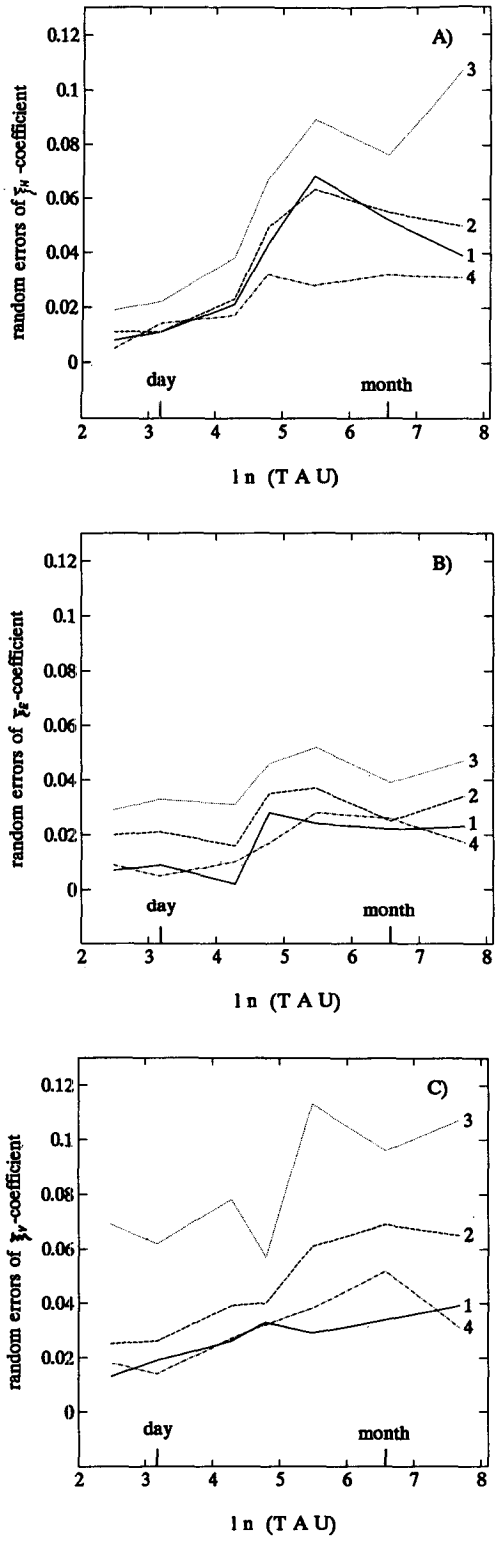

FIG. 11. Random errors of $\xi_H(\tau)$ (a), $\xi_E(\tau)$ (b), and $\xi_V(\tau)$ (c) coefficients as functions of temporal-averaging period for winter (1), spring (2), summer (3), and autumn (4).

TABLE 7. Uncertainties (in percent of $\xi - 1$) of temporal-averaging formulas (6).

Season	Range	ξ_H	ξ_E	ξ_V
Winter (JFM)	1–5 d	9	8	6
	5 d–3 mo	7	5	6
Spring (AMJ)	1–5 d	10	13	13
	5 d–3 mo	11	10	11
Summer (JAS)	1–5 d	21	18	23
	5 d–3 mo	24	26	25
Autumn (OND)	1–5 d	4	6	5
	5 d–3 mo	4	4	4

eraging leads to the significant changes of the heat and momentum fluxes. For example, for $\tau = 240$ h and $2r = 640$ km $\xi_H(\tau, r)$, values are more than 2.0. For latent heat flux $\xi_E(\tau, r) > 2$ already for $\tau = 120$ h and $2r = 560$ km. The two-dimensional distribution of the coefficient $\xi_E(\tau, r)$ appears to be much more complicated than for $\xi_H(\tau, r)$. Thus, values of $\xi_E(\tau, r)$ indicate local maximums at $\tau = 80$ h, $2r = 120$ km, and $\tau = 200$ h, $2r = 480$ km. Generally, Figs. 10a and 10b demonstrate that joint space–time averaging is more complicated than the linear combination of both temporal and spatial averaging and cannot be reproduced on the basis of only spatial or only temporal estimates. Actually, all the results concerned with joint space–time averaging should be considered as preliminary estimates because the quantity of data was very limited. Figure 10 should not be taken as universal for all the cases like the similar estimates for only time or only space averaging (Figs. 4 and 7).

5. The accuracy and errors

In previous sections, no information was given about the accuracy and uncertainties of formulas (6)–(9). This problem is very important for the applications of these formulas to practical calculations and modeling. Estimates of uncertainties and errors of the averaging formulas (6)–(9) are based on the comparison of averaged fluxes, calculated using the formulas according to (10), with direct estimates on the basis of sampled data. Defining the estimates of fluxes under the classical approach as $\hat{Q}$ and the estimates on the basis of sampled data as Q, it is easy to obtain a direct estimate of $\xi^{(d)}$ as

$$\xi^{(d)} = Q/\hat{Q}. \tag{13}$$

The resultant $\xi^{(d)}$ and $\xi(V, \delta T)$, taken from (6)–(9), residual is

$$R_\xi^2 = \overline{(\xi^{(d)} - \xi)^2}, \tag{14}$$

where the overbar indicates averaging over all individual estimates for a fixed averaging period or fixed averaging radius.

Random errors (14) of $\xi(\tau)$ coefficients were calculated for four seasons. Results are presented in Fig.

11, and Table 7 gives averages of errors for two ranges of τ (1–5 days and 5 days–3 months) expressed in terms of percent in relation to ($\xi - 1$) values. For all of fluxes, errors increase considerably in summer, which may be related to smaller absolute values of fluxes, and relatively high probability of stable stratification ($\delta T > 0$) as well. The smallest errors of ξ_H, ξ_E, and ξ_V were obtained for winter and autumn. For all seasons, $\xi_H(\xi)$ and $\xi_E(\xi)$ curves in Fig. 11 indicated a definite break in the vicinity of $\tau = 5$ days. Thus, we can take less than 10%–15% accuracy for formulas (6) for all the seasons, except summer and maybe late spring, when the values of energy fluxes are small, or stratification is stable.

The data were too limited to describe seasonal uncertainties for spatial averaging. Consequently, Fig. 12 and Table 8 show the annual mean errors of formulas (8) and (9) in the same terms as Fig. 11 and Table 7. Errors of spatial-averaging formulas appear to be dependent on wind speed. Thus, Fig. 12 shows error estimates for two ranges of wind speed ($V < 9$ m s^{-1} and $V > 9$ m s^{-1}). For small and moderate winds, errors of $\xi_H(r)$ and $\xi_E(r)$ increase with spatial-averaging scale. For strong winds (thin lines in Fig. 12) the highest errrors are observed for $2r < 280$ km and $2r > 600$ km. In contrast with $\xi_H(r)$ and $\xi_E(r)$, errors of $\xi_V(r)$ increase with wind speed for strong winds and appear to have complicated behavior with wind speed for small and moderate winds. The maximum of uncertainties (10%–15%) corresponds to the correction coefficient of latent heat fluxes. This is comparable with the accuracy of the formulas for the temporal averaging (Table 7).

TABLE 8. Annual mean uncertainties (in percent of $\xi - 1$) of spatial-averaging formulas (8, 9).

Range	ξ_H	ξ_E	ξ_V
0–280 km	6	9	5
280–560 km	7	12	8
560–800 km	7	15	9

Figure 13 illustrates the attempt to calculate the spatial distribution of sensible and latent fluxes in the northwest Atlantic from 8 February until 7 March 1988. Panels (a) and (d) were obtained by the calculation of fluxes on the basis of individual observations. Then fluxes were interpolated on the 2.5° by 2.5° net-

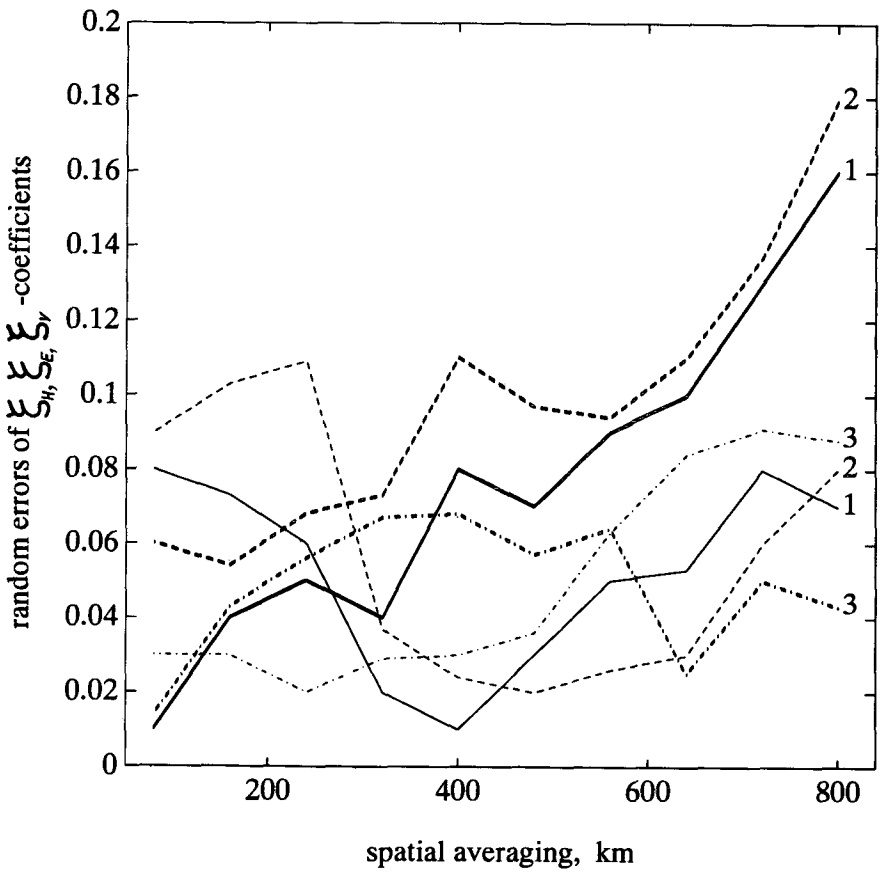

FIG. 12. Random errors of $\xi_H(r)$ (1), $\xi_E(r)$ (2), and $\xi_V(r)$ (3) coefficients as functions of spatial-averaging scale for $V < 9$ m s^{-1} (bold lines) and $V > 9$ m s^{-1} (light lines).

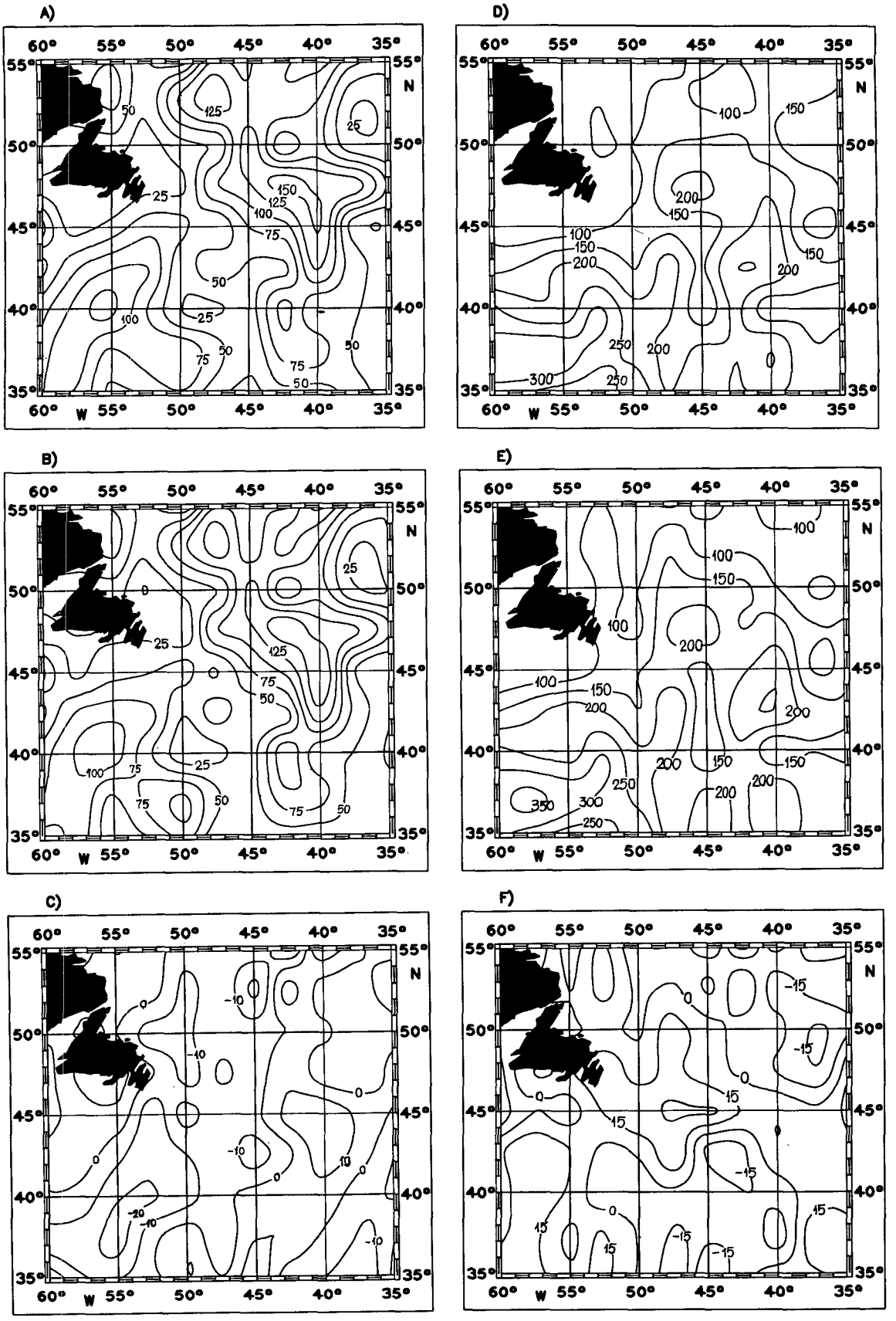
A)
B)
C)
D)
E)
F)
60° 55° 50° 45° 40° 35°
55° 50° 45° 40° 35°
N
W

work and plotted. Panels (b) and (e) were calculated by formulas (10) on the basis of meteorological information previously averaged on the same network. All of the most important features appear to be presented in panels 13 (b) and (e) in comparison with (a) and (d). Errors [panels (c) and (f)] are less than 10% of the real flux in most cases. Mean square error is about 8 W m^{-2} for sensible flux and less than 15 W m^{-2} for latent flux. The most significant errors were obtained in the region of well-known (Budyko 1963; Bunker 1976; Esbensen and Kushnir 1981; Isemer and Hasse 1987, Isemer et al. 1989) maximum fluxes southward of Newfoundland. It is interesting to note that negative errors of Q_H calculations correspond here to positive errors of Q_E that reflect different laws of $\xi(V, \delta T)$ and $\xi(V, \delta e)$ in formulas (6)–(9).

The typical relative error of 10% [in terms of $(\xi - 1)$] corresponds to absolute errors of ξ_H, ξ_E, and ξ_V of less than 0.1. This error is comparable to or less than natural dispersions of the averaging correction coefficients (Marsden and Pond 1983; Gulev and Ukrainsky 1989). Thus, we can take this accuracy for practical application of the formulas (6)–(9) to climatological calculations and modeling.

6. Discussion

Earlier (see Introduction) we noted that there are two problems in the bulk formula applications for energy exchange estimates. Accordingly, two types of transfer coefficient parameterizations were constructed by different authors. The first type is connected with the principal physical laws of the atmospheric boundary layer and based on direct flux measurements (Friehe and Schmitt 1976; Hasse 1970; Pond et al. 1974; Smith and Banke 1975; Large and Pond 1981; etc.) or on theoretical treatment (Krugermeyer 1976; Liu et al. 1979; Ariel et al. 1981; etc). Different schemes were compared by Blanc (1985), who found a large range in the transfer coefficient behavior. Another type of parameterization is applied to climatological calculations based on summaries of different coefficients (Bunker 1976) or on the different inverse principals in respect to heat balance of different regions (Budyko 1963, 1974; Bunker et al. 1982; Efimov et al. 1985; Isemer et al. 1989). Although this type of parameterization takes into account averaging problems indirectly, the main idea of all of these parameterizations was to construct the coefficients that can lead to the most realistic results on the basis of specific datasets for the specific regions and specific resolution.

Our study (and similar works that were referred to in the Introduction) is intermediate between these two types of investigations. It suggests the possibility of changing the original bulk aerodynamical formulas in climatological calculations and modeling. This is significant because of the fact that the number of datasets already averaged for different space and time scales has increased considerably during the last several years. Efforts of the Tropical Oceans and Global Atmosphere Experiment, the World Ocean Circulation Experiment, the European Centre for Medium-Range Weather Forecasts, and other scientific programs and groups (Jones et al. 1994) show that the number of datasets of this type will also increase in the future. Very often the initial basis of averaged data in the form of sampled observations is not available immediately or one needs to take essential efforts to work with individual reports. Sometimes it is useful to combine different datasets (SST, air temperature, wind speed) from different sources, produced with different spatial and temporal resolution. Our results can be used in experiments with circulation models, which also need to calculate grid- and time-averaged fluxes. Our results yield the possibility of using the original bulk formulas with averaging correction for all of these properties.

The question of universal applicability of these results should be evaluated. This question should be considered both for different regions and historical periods as well as for different transfer coefficients schemes. The regional aspect appears to be much more connected with integral statistical characteristics of different regions than with their mean meteorological parameters. From this point of view, the tropics and mid-latitudes, for example, can be much more comparable, than, say, the eastern and western parts of the oceans. Nevertheless, it is necessary to study the statistical properties of different areas on different scales. Some efforts in this direction already have been taken (Gulev 1994). The problem of different bulk schemes should be discussed in terms of the covariances of coefficients with V, δT, and δe, and appears to be dependent on the significance of each of last four terms on the right-hand side of (2), which will be considered in the Appendix.

Investigations of the influence of averaging effects on the long-term variability are also significant. Marsden and Pond (1983) demonstrated clear differences between climatic spectra of heat and momentum fluxes, calculated under classical and sampling approaches. They showed a pronounced annual maximum in spectral power of $C_p\rho_a(\langle C_T V \delta T\rangle - \langle C_T\rangle\langle V\rangle\langle \delta T\rangle)$, which coincides with our results (see section 4). The power of different harmonics of sampling and classical spectra, according to Marsden

FIG. 13. Mean sensible (a)–(c) and latent (d)–(f) heat fluxes (W m^{-2}) for the period from 8 February 1988 till 7 March 1988. (a), (d) Fluxes have been calculated using sampled observations and then interpolated. (b), (e) Fluxes have been calculated using formulas (10) on the basis of previously averaged data. (c), (f) Differences between (b), (e) and (a), (d), respectively.

and Pond (1983), were contradictory. It is possible that parameters of long-term trends of fluxes will also change (maybe even in terms of sign), if one goes from classical estimates to sampling calculations. This is also a suggested line of future investigation.

Acknowledgments. I wish to acknowledge discussions with Prof. S. S. Lappo and Prof. S. P. Malevsky concerning applications of the bulk formulas to climatological estimates. Discussions with H.-J. Isemer of IFM (Kiel) concerning this work were very helpful. I also wish to thank both of the reviewers for very constructive comments. This study was supported by the Department of the World Ocean of the State Hydrometeorology Committee of the USSR under Grant 1989/1.6.1 (Sections).

APPENDIX

The Behavior of Correlation Terms

In section 4 we did not discuss the structure of the right-hand side of (2), although the behavior of the correlation terms is very important in the assessment of the difference between the classical and sampling methods. Figure A1 shows the behavior of the individual correlation terms (2) on synoptic scales for temporal averaging. The monotonic decrease is typical only for the terms $\langle \delta T\rangle_\tau\langle C'_T V'\rangle_\tau$, $\langle \delta e\rangle_\tau\langle C'_E V'\rangle_\tau$, $\langle V\rangle_\tau \langle C'_T\delta T'\rangle_\tau$, and $\langle V\rangle_\tau\langle C'_E\delta e'\rangle_\tau$ containing the correlations of the transfer coefficients with the individual parameters. The maximum of $\langle C_T\rangle_\tau\langle \delta T'V'\rangle_\tau$ is observed at τ = 3–5 d, which agrees with the increase of δT and V at the synoptic scale. The covariance $\langle C'_T\delta T'V'\rangle$ is practically constant in the range of 3 $< \tau <$ 240 h; and the terms $\langle C'_E\delta e'V'\rangle_\tau$ and $\langle C'_E\delta e'V'\rangle_\tau$ increase from zero and negative values to 1.0–1.5. With the increase of τ, the contribution of individual correlation terms to $\langle C_T\delta TV\rangle_\tau$ varies significantly. In the range $3 < \tau < 24$ h, the largest contribution comes from $\langle \delta T\rangle_\tau\langle C'_T V'\rangle_\tau$, $\langle V\rangle_\tau \langle C'_T\delta T'\rangle_\tau$ for Q_H and from $\langle \delta e\rangle_\tau\langle C'_E V'\rangle_\tau$, $\langle V\rangle_\tau \langle C'_E\delta e'\rangle_\tau$ for Q_E. When τ = 3 d, the contribution from the correlations $\langle \delta T'V'\rangle_\tau$, $\langle C'_T\delta T'V'\rangle_\tau$, $\langle \delta e'V'\rangle_\tau$, and $\langle C'_E\delta e'V'\rangle_\tau$ increases. The seasonal evolution of the individual correlation terms with $3 < \tau < 240$ h is shown in Fig. A2. Although all terms have a pronounced seasonal dependence, the behavior of individual covariances depends on the season of the year. During the fall and winter a local maximum of $\langle C_T\rangle_\tau\langle \delta T'V'\rangle_\tau$ is observed when τ = 1–3 d. In summer this maximum disappears or shifts to τ = 5 d, which corresponds to the summer weakening of the synoptic variability. For the term $\langle C'_T\delta T'V'\rangle_\tau$, a minimum, corresponding to τ = 3–5 days, can be observed in fall and winter.

It is interesting to compare our individual correlation term estimates with the results of other authors to study the sensitivity of coefficients (2) to different bulk schemes. Simmonds and Dix (1989) presented similar calculations on the basis of numerical experiments in zonally averaged form. From Simmonds and Dix (1989) $\langle C_T\rangle_\tau\langle \delta T'V'\rangle_\tau$ gives a negative contribution in January. Figure A2 shows positive January values, but already in February this covariance is significantly negative. The positive contributions from the term $\langle V\rangle_\tau\langle C'_T\delta T'\rangle_\tau$ in winter and summer are obtained by Simmonds and Dix (1989) and the present study. This term was significantly positive in the Esbensen and Reynolds (1981) study, where the Liu et al. (1979) scheme for transfer coefficients has been used. So, we can take these two covariances ($\langle C_T\rangle_\tau\langle \delta T'V'\rangle_\tau$ and $\langle V\rangle_\tau\langle C'_T\delta T'\rangle_\tau$) as the most important contributors for the differences between classical and sampling

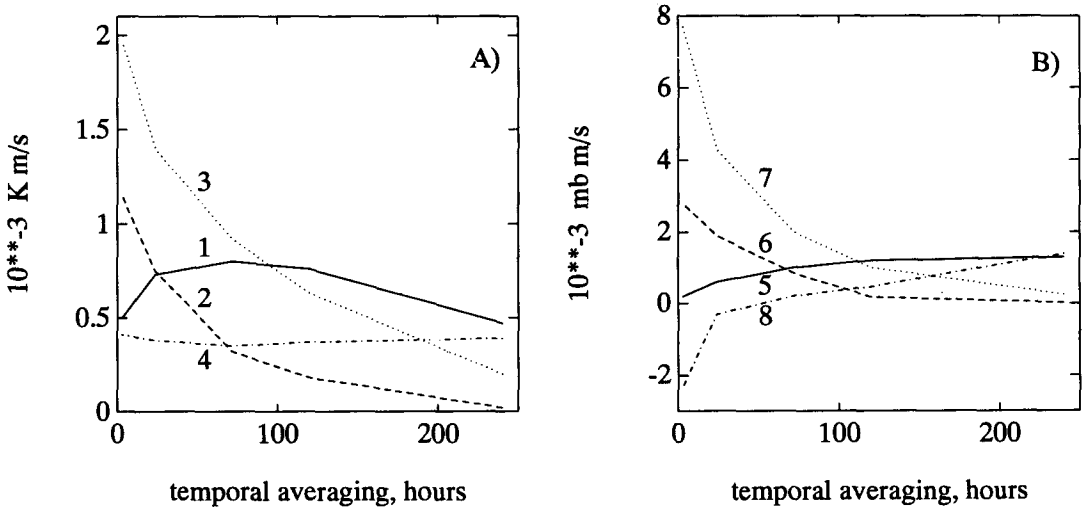

FIG. A1. The behavior of the individual correlation terms for sensible flux (a) and latent flux (b) in dependence on temporal-averaging scales: (1) $\langle C_T\rangle\langle \delta T'V'\rangle$, (2) $\langle \delta T\rangle\langle C'_T V'\rangle$, (3) $\langle V\rangle\langle C'_T\delta T'\rangle$, (4) $\langle C'_T\delta T'V'\rangle$, (5) $\langle C_E\rangle\langle \delta e'V'\rangle$, (6) $\langle \delta e\rangle\langle C'_E V'\rangle$, (7) $\langle V\rangle\langle C'_E\delta e'\rangle$, and (8) $\langle C'_E\delta e'V'\rangle$.

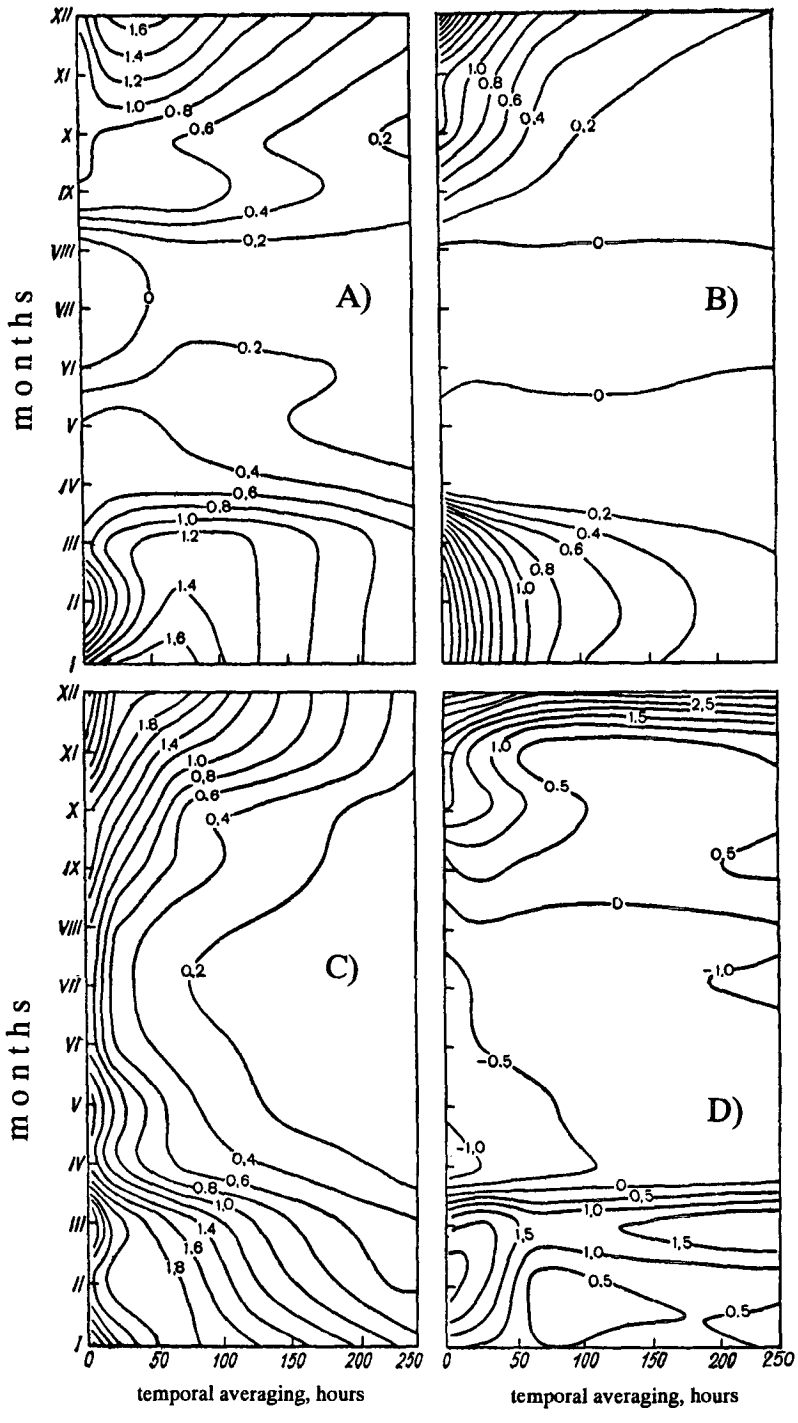

FIG. A2. Seasonal dependence of individual correlation terms as a function of temporal-averaging scale: (a) $\langle C_T \rangle \langle \delta T'V' \rangle$, (b) $\langle \delta T \rangle \langle C_T'V' \rangle$, (c) $\langle V \rangle \langle C_T' \delta T' \rangle$, and (d) $\langle C_T' \delta T'V' \rangle$.

methods. Kondo (1972), using the linear dependence of transfer coefficients on wind speed, also found that covariances $\langle C_T \rangle_\tau \langle \delta T'V' \rangle_\tau$ and $\langle C_E \rangle_\tau \langle \delta e'V' \rangle_\tau$, which are independent of the kind of scheme used for transfer coefficients, give the largest contribution to $\langle C_T \delta TV \rangle_\tau$ and $\langle C_E \delta eV \rangle_\tau$. In principle, we can talk about qualitative coincidence of our estimates with Simmonds and Dix (1989) and Esbensen and Reynolds (1981).

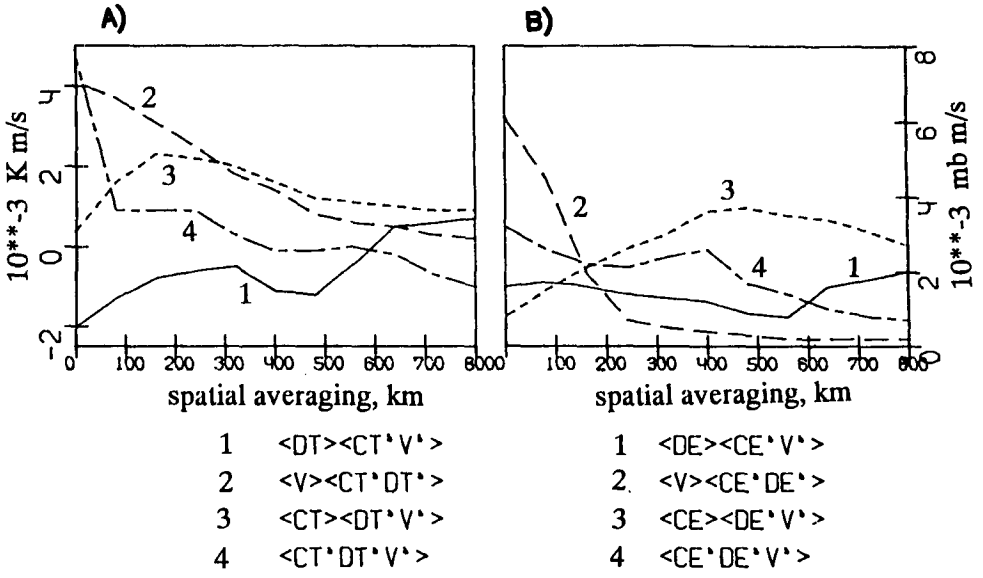

FIG. A3. The behavior of individual correlation terms in dependence of spatial-averaging scales for (a) sensible heat flux and (b) latent heat flux.

Individual correlation term estimates for spatial averaging are shown in Fig. A3. Monotonic decreases were observed only for the terms $\langle V\rangle_r\langle C'_T\delta T'\rangle_r$, $\langle C'_T\delta T'V'\rangle_r$, $\langle V\rangle_r\langle C'_E\delta e'\rangle_r$, which give the largest contributions at the mesometeorological scales. The behavior of $\langle C_T\rangle_r\langle\delta T'V'\rangle_r$ and $\langle C_E\rangle_r\langle\delta e'V'\rangle_r$ has local maxima for $2r$ = 180–300 km and $2r$ = 420–560 km, respectively. Starting from $2r$ = 300–400 km, terms $\langle C_T\rangle_r\langle\delta T'V'\rangle_r$ and $\langle C_E\rangle_r\langle\delta e'V'\rangle_r$ give more than 50%–60% contribution to $\langle C_T\delta TV\rangle$ and $\langle C_E\delta eV\rangle$. These two terms on the right-hand side of (2) also appear to be independent of the parameterization of C_T and C_E and will be preserved on the right-hand side of (2) even under C_T = Const and C_E = Const. Thus, we can see, that at least for $2r > 300$ km (less than 3° of latitude) the averaging influence on heat flux estimates does not appear to be strongly sensitive to the choice of bulk scheme and is mostly determined by the correlation between V and δT.

REFERENCES

Adamec, D., and R. L. Elsbery, 1984: The use of mean atmospheric forcing in an ocean mixed-layer model. *J. Phys. Oceanogr.*, **14**, 1670–1676.

Ariel, N. Z., R. S. Bortkovskiy, S. P. Malevsky, and A. V. Murashova, 1981: Sensible, latent and momentum flux calculations over the sea. Methodical comments, Main Geophysical Observatory, Leningrad, 55 pp.

Blanc, T. V., 1985: Variation on bulk-derived surface flux, stability and roughness due to the use of different transfer coefficient schemes. *J. Phys. Oceanogr.*, **15**, 650–669.

Bortkovskiy, R. S., 1983: *Atmosphere-Ocean Heat and Moisture Exchange at Storm Conditions.* Gidrometeouzdat, Leningrad, 160 pp.

Budyko, M. I., 1963: *Atlas of Heat Balance of the Earth.* Academic Sciences of the USSR, 69 pp.

——, 1974: *Climate and Life. Int. Geophys. Ser.*, Vol. 18, Academic Press, 508 pp.

Bunker, A. F., 1976: Computations of surface energy flux and annual air–sea interaction cycles of the North Atlantic Ocean. *Mon. Wea. Rev.*, **104**, 1122–1140.

——, H. Charnock, and R. A. Goldsmith, 1982: A note on the heat balance of the Mediterranean and Red Seas. *J. Mar. Res.*, **40**(Suppl.), 73–84.

Cardone, J. S., J. G. Greenwood, and M. A. Cane, 1990: On trends in historical marine wind data. *J. Climate*, **3**, 113–127.

Efimov, V. V., N. A. Timofeev, I. V. Kurzeevsky, and E. N. Sychov, 1985: The estimate of the coefficients of the heat and moisture transfer between the ocean and atmosphere. *Izv. Acad. Sci. USSR, Atmos. Oceanic Phys.*, **21**, 735–743.

Esbensen, S. K., and V. Kushnir, 1981: The heat budget of the global oceans: An atlas based on estimates from marine surface observations. Oregon State University Climatic Research Institute Rep. No. 29, 27 pp. + 188 figs.

——, and R. W. Reynolds, 1981: Estimating monthly averaged air–sea transfers of heat and momentum using the bulk aerodynamic method. *J. Phys. Oceanogr.*, **11**, 457–465.

Fissel, D. V., S. Pond, and M. Miyake, 1977: Computation of surface fluxes from climatological and synoptic data. *Mon. Wea. Rev.*, **105**, 26–36.

Frihe, C. A., and K. F. Schmitt, 1976: Parameterization of air–sea interface fluxes of sensible heat and moisture by the bulk aerodynamic formulas. *J. Phys. Oceanogr.*, **6**, 801–809.

Garstang, M., 1965: Distribution and mechanism of energy exchange between the tropical oceans and the atmosphere. Pap. Dept. of Meteorology, Florida Univ. Rep. No. DA-AMC-28-043-64-05, 46 pp.

Gavrilin, B. L., and A. S. Monin, 1969: On calculations of climatic correlations, using numerical atmospheric models. *Izv. Acad. Sci. USSR, Atmos. Oceanic Phys.*, **6**, 659–665.

Gilhousen, D. B., 1987: A field evaluation of NDBC moored buoy Winds. *J. Atmos. Oceanic Technol.*, **4**, 94–104.

Grachov, A. A., and G. N. Panin, 1984: Sensible and latent heat flux parameterization over water surface under natural conditions. *Izv. Acad. Sci. USSR, Atmos. Oceanic Phys.*, **20**, 364–371.

Gulev, S. K., 1994: Long-term variations of statistical characteristics of ocean–atmosphere exchange processes. *Izv. Acad. Sci. USSR, Atmos. Oceanic Phys.*, **30**, in press.

——, and A. V. Kolinko, 1987: Interpretation of polygonal hydrometeorological data from the oceanic energy active regions. *Meteorol. Hydrol.*, **12**, 54–61.

——, and V. V. Ukrainsky, 1989: The role of different time-scales in ocean–atmosphere energy exchange processes. *Izv. Acad. Sci. USSR, Atmos. Oceanic Phys.*, **25**, 675–687.

——, and A. V. Kolinko, 1990: Synoptic variability of the ocean–atmosphere heat and water exchange in midlatitudinal ocean frontal zones. *Meteorol. Hydrol.*, **9**, 85–93.

——, A. Y. Ivanov, A. V. Kolinko, S. S. Lappo, and E. G. Morozov, 1991: The ATLANTEX-90 Experiment. *Meteorol. Hydrol.*, **5**, 54–70.

Hanava, K., and Y. Toba, 1987: Critical examination of estimation methods of long-term mean air–sea heat and momentum transfers. *Ocean–Air Interactions*, **1**, 79–93.

Hasse, L., 1970: On the determination of vertical transport of momentum and heat in the atmospheric boundary layer at sea. Tech. Rep. No. 188, School of Oceanography, Oregon State University, 55 pp.

Husby, D. M., 1980: A comparison of surface heat flux estimates from ocean weather station V and merchant vessels in its vicinity in the western North Pacific region, 1956–1970. *J. Phys. Oceanogr.*, **10**, 971–975.

Isemer, H.-J., 1993: On the homogeneity of surface wind speed records from ocean weather stations. Tech. Rep., Institute für Meereskunde, 89 pp. [Available from Institut für Meereskunde, Dusternbrooker Weg 20, D-24105 Kiel, Germany.]

——, and L. Hasse, 1987: *The Bunker Climate Atlas of the North Atlantic Ocean.* Vol. 2, *Air–sea Interactions.* Springer-Verlag, 252 pp.

——, and ——, 1991: The scientific Beaufort equivalent scale: Effects on wind statistics and climatological air–sea flux estimates in the North Atlantic Ocean. *J. Climate*, **4**, 819–836.

——, and R. Lindau, 1992: Trends in marine surface wind speeds: Ocean weather ships versus voluntary observing ships. *Second Int. Conf. on Modelling of Global Climate Change and Variability*, Hamburg, Max-Plank Institute für Meteorologie, 26.

——, J. Willebrand, and L. Hasse, 1989: Fine adjustment of large scale air–sea energy flux parameterizations by direct estimates of ocean heat transport. *J. Climate*, **2**, 1173–1184.

Jones, C. S., D. Legler, and J. J. O'Brien, 1994: Variability of surface fluxes over the Indian Ocean, 1960–1989. *The Atmosphere–Ocean System*, in press.

Kondo, J., 1972: Applicability of micrometeorological transfer coefficient to estimate the long-period means of fluxes in air–sea interface. *J. Meteor. Soc. Japan*, **50**, 570–576.

——, 1975: Air–sea bulk transfer coefficients in diabatic conditions. *Bound.-Layer Meteor.*, **9**, 91–112.

Kraus, E. B., and R. E. Morrison, 1966: Local interactions between the sea and the air at monthly and annual time scales. *Quart. J. Roy. Meteor. Soc.*, **92**, 114–127.

Krugermeyer, L., 1976: Vertical transport of momentum, sensible and latent heat from profiles at the tropical Atlantic during ATEX. *"Meteor" Forschungsergeb*, **11**, 51–77.

Lander, M., J. C. Sadler, J. Maliekal, and A. Hori, 1989: Tropical wind stress from time-averaged winds. *J. Appl. Meteor.*, **28**, 904–912.

Lappo, S. S., R. V. Ozmidov, Y. A. Volkov, S. K. Gulev, A. V. Kolinko, and S. P. Malevsky, 1989: The SECTIONS-NEW-FOUEX-88 Experiment. *Meteorol. Hydrol.*, **9**, 67–77.

Large, W. G., and S. Pond, 1981: Open ocean momentum flux measurements in moderate to strong winds. *J. Phys. Oceanogr.*, **11**, 324–336.

——, and ——, 1982: Sensible and latent heat fluxes over the ocean. *J. Phys. Oceanogr.*, **12**, 463–482.

Larin, D. A., and G. N. Panin, 1985: The correlation between meteorological parameters influence on the calculations of evaporation and heat exchange over the Kaspy sea. *Water Resour.*, **5**, 68–75.

Legler, D., 1991: Errors in five-day mean surface wind and temperature conditions due to inadequate sampling. *J. Atmos. Oceanic Technol.*, **8**, 705–712.

Lindau, R., H.-J. Isemer, and L. Hasse, 1990: Towards time-dependent calibration of historical wind observations at sea. *Trop. Ocean–Atmos. Newslett.*, **54**, 7–12.

Liu, W. T., and T. Blanc, 1984: The Liu, Katsaros and Businger (1979) bulk atmospheric flux computational iteration program in FORTRAN and BASIC. NRL Memo. Rep. 5291, Naval Research Laboratory, Washington, DC, 17 pp.

——, K. B. Katsaros, and J. A. Businger, 1979: Bulk parameterization of air–sea exchanges of heat and water vapor including the molecular constraints at the interface. *J. Atmos. Sci.*, **36**, 1722–1735.

Louis, J.-F., 1979: A parametric model of vertical eddy fluxes in the atmosphere. *Bound.-Layer Meteor.*, **17**, 187–202.

Mahrt, L., 1987: Grid-averaged surface fluxes. *Mon. Wea. Rev.*, **115**, 1550–1560.

Marsden, R. F., and S. Pond, 1983: Synoptic estimates of air–sea fluxes. *J. Mar. Res.*, **41**, 349–373.

Peterson, E. W., and L. Hasse, 1987: Did the Beaufort scale or the wind climate change? *J. Phys. Oceanogr.*, **17**, 1071–1074.

Pond, S., D. B. Fissel, and C. A. Paulson, 1974: A note on bulk aerodynamic coefficients for sensible heat and moisture fluxes. *Bound.-Layer Meteor.*, **6**, 333–339.

Ramage, C. S., 1984: Can shipboard measurements reveal secular changes in tropical air–sea heat flux? *J. Climate Appl. Meteor.*, **23**, 187–193.

Reed, R. K., 1985: An estimate of the climatological heat fluxes over the tropical Pacific Ocean. *J. Climate Appl. Meteor.*, **24**, 833–840.

Robinson, G. D., 1966: Another look at some problems of the air–sea interface. *Quart. J. Roy. Meteor. Soc.*, **92**, 451–465.

Saunders, P. M., 1976: On the uncertainty of wind stress curl calculations. *J. Mar. Res.*, **34**, 155–160.

Simmonds, I., and M. Dix, 1989: The use of mean atmospheric parameters in the calculation of modeled mean surface heat fluxes over the world's oceans. *J. Phys. Oceanogr.*, **19**, 205–215.

Smith, S. D., and E. G. Banke, 1975: Variation of the sea surface drag coefficient with wind speed. *Quart. J. Roy. Meteor. Soc.*, **101**, 665–673.

Thompson, K. R., Marsden R. F., and Wright D. G., 1983: Estimation of low-frequency wind stress fluctuations over the open ocean. *J. Phys. Oceanogr.*, **13**, 1003–1011.

Weare, B. C., 1989: Uncertainties in estimates of surface heat fluxes derived from marine reports over the tropical and subtropical oceans. *Tellus*, **41A**, 357–370.

——, and P. T. Strub, 1981: The significance of sampling biases on calculated monthly mean oceanic surface heat fluxes. *Tellus*, **33**, 211–224.

Willebrand, J., 1978: Temporal and spatial scales of the wind field over the North Pacific and North Atlantic. *J. Phys. Oceanogr.*, **8**, 1080–1094.

Wright, D. G., and K. R. Thompson, 1983: Time averaged forms of nonlinear stress low. *J. Phys. Oceanogr.*, **13**, 341–345.